Astronomical Contributions from the University of Manchester

JEREMIAH HORROCKS' OBSERVATORY,
MOOR PARK, PRESTON.

SERIES III, No. 128

THREE COLOUR PHOTOELECTRIC PHOTOMETRY OF THE MOON

by

G. L. ROBERTS

Department of Astronomy
University of Manchester

The research reported in this document has been sponsored by the Air Force Cambridge Research Laboratories under Contract No. AF 61(052)-882, through the European Office of Aerospace Research (OAR), United States Air Force.

July 1965

THREE COLOUR PHOTOELECTRIC PHOTOMETRY OF THE MOON

by

G. L. ROBERTS

Department of Astronomy
University of Manchester

ABSTRACT

This report describes experiments attempting to measure the time variation of the luminescence of the lunar surface material, assuming a luminescence band for the surface material similar to that stimulated in certain meteorite samples in the laboratory. The two instruments used are described briefly and a discussion of the results obtained, both in the laboratory and at the telescope, is given.

CONTENTS

Page

ABSTRACT

SECTION I

Introduction 1

SECTION II

An Astronomical Photoelectric Photometer 5

SECTION III

The Three Beam Photoelectric Photometer 29

SECTION IV

Results and Discussion 43

SECTION I

INTRODUCTION

The luminescence of minerals, exposed on the lunar surface, stimulated by high energy radiation and charged particle streams from the Sun was first suggested by Link (1), as an explanation of excess light found in certain areas on the Moon. This excess light was further detected by Kozyrev (2) and Dubois (3) using spectrographic methods and by Grainger (4) using spectrophotoelectric methods. Discrepancies in their results were attributed to time variations of the luminescence.

The discovery in the laboratory of strong luminescence in certain meteorite samples (which could possibly exist on the lunar surface) by Geake et al (5) suggested a new line of study. Using narrow passband filters centred "on" and "off" the luminescence band one studies the time variations of the luminescence in an attempt to correlate variations with solar activity.

With this in mind a programme of photographic and photoelectric study, sponsored by the United States Air Force under Grant No. AF EOAR

64-72 *, was started in the Autumn of 1963 by the Department of Astronomy of the University of Manchester working at Pic-du-Midi Observatory in France. This report summarises the photoelectric study carried out by the author (a full account is given in the author's thesis (7)). The photographic study is described elsewhere (6).

A review of previous work on the subject of lunar luminescence (7) showed that both spectrographic (2, 3) and spectrophotoelectric (4) methods were unsatisfactory for the continuous monitoring of short time variations (of the order of minutes (6)) in the luminescence. Continuous monitoring is essential if one if to correlate specific lunar events with specific solar events. Observations of luminescence during a lunar eclipse would also be useful in distinguishing between stimulation by photons or by charged particles since their eclipse shadow patterns would differ.

A method was therefore required whereby the moonlight was accurately measured in three wavelength regions (one "on" and two "off" the luminescence band). This was achieved using narrow passband filters and photoelectric detectors.

---

* Now Contract AF 61(052)-882

The instrument used to carry out preliminary investigations was a single beam photoelectric photometer described in the following section. Useful laboratory experiments were carried out with this instrument and the results obtained at the telescope show the limitations of the single beam instrument.

The only way of removing the effect of atmospheric scintillation from the measured signals is to take the simultaneous ratios of the signals. The three beam photoelectric photometer, described in Section III, allows one to do this.

Laboratory experiments carried out with the three beam photometer are described in Section III and measurements on the eclipsed Moon of 25th June, 1964 and on the uneclipsed Moon of 30th June, and 1st July are discussed in Section IV. The report concludes with a discussion of recent improvements made and a discussion of future observing plans.

SECTION II

AN ASTRONOMICAL PHOTOELECTRIC PHOTOMETER

A method of measuring the time variation of lunar luminescence using narrow passband filters has been suggested. This section discusses photometric considerations leading to the design of a photoelectric photometer to do this task, and describes a single beam photoelectric photometer used to carry out preliminary investigations. The variation of the signal to noise ratio of a photomultiplier with applied voltage is described, and the results obtained at the telescope are collected at the end of this section.

Photometric Accuracy Considerations

If one isolates a wavelength region in the image of a selected area of the Moon, formed in the focal plane of a telescope, and one measures photoelectrically the continuous variation of this signal with time, then the measured signal will consist of three components: (i) a component $S(\lambda, t)$ due to scattered sunlight, (ii) a component $L(\lambda, t)$ due to luminescence and (iii) a component $T(\lambda, t)$ due to atmospheric scintillation and transparency changes. The measured signal is therefore:

$$\left[S(\lambda, t) + L(\lambda, t) \right] T(\lambda, t)$$

where λ represents wavelength, and t time.

If one measures in two wavebands centred on λ_1 and λ_2, at times t_1 and t_2, respectively, the signals become:

$$\left[S(\lambda_1, t_1) + L(\lambda_1, t_1) \right] T(\lambda_1, t_1) \quad \text{and}$$

$$\left[S(\lambda_2, t_2) + L(\lambda_2, t_2) \right] T(\lambda_2, t_2) \quad .$$

From which it would be difficult to detect small relative changes in the signals due to luminescence, because changes in T could be of the order of five per cent and further changes in the signals could be caused by bad guidance.

The only way to eliminate completely the effect of the atmosphere is to take the ratio of the simultaneous measurements in each waveband. This can be done by either measuring each signal simultaneously and taking the ratio subsequently or by measuring the ratio directly using a ratio recorder, the latter method having an accuracy greater by a factor $\sqrt{2}$. The ratio method also compensates for guidance errors. The only assumption made is that the scintillation and transparency changes are coherent in the two

wavelength regions considered, which is a reasonable assumption in view of previous work by Hiltner (8) and others (9). The justification of this assumption is also shown by results obtained at the telescope with the three-beam photoelectric photometer described later.

If, then, we take the simultaneous ratio of the signals we obtain:

$$R = \frac{L_1 + S_1}{L_2 + S_2}$$

[Where the suffix 1 is short for (λ_1, t_1) etc.]

In order to see the fractional change in this ratio, caused by the time variation of luminescence, we differentiate and divide by R giving:

$$\frac{\delta R}{R} = \frac{\delta L_1}{L_1 + S_1} - \frac{\delta L_2}{L_2 + S_2} \qquad 2.1$$

where S_1 and S_2 are assumed constant.

The behaviour of $\frac{\delta R}{R}$ depends on the relative importance of the two terms on the right-hand side of equation 2.1, and in order to show this relative importance we consider the case when λ_1 is centred on the peak of a luminescence band and λ_2 is centred on the minimum (Figure 1).

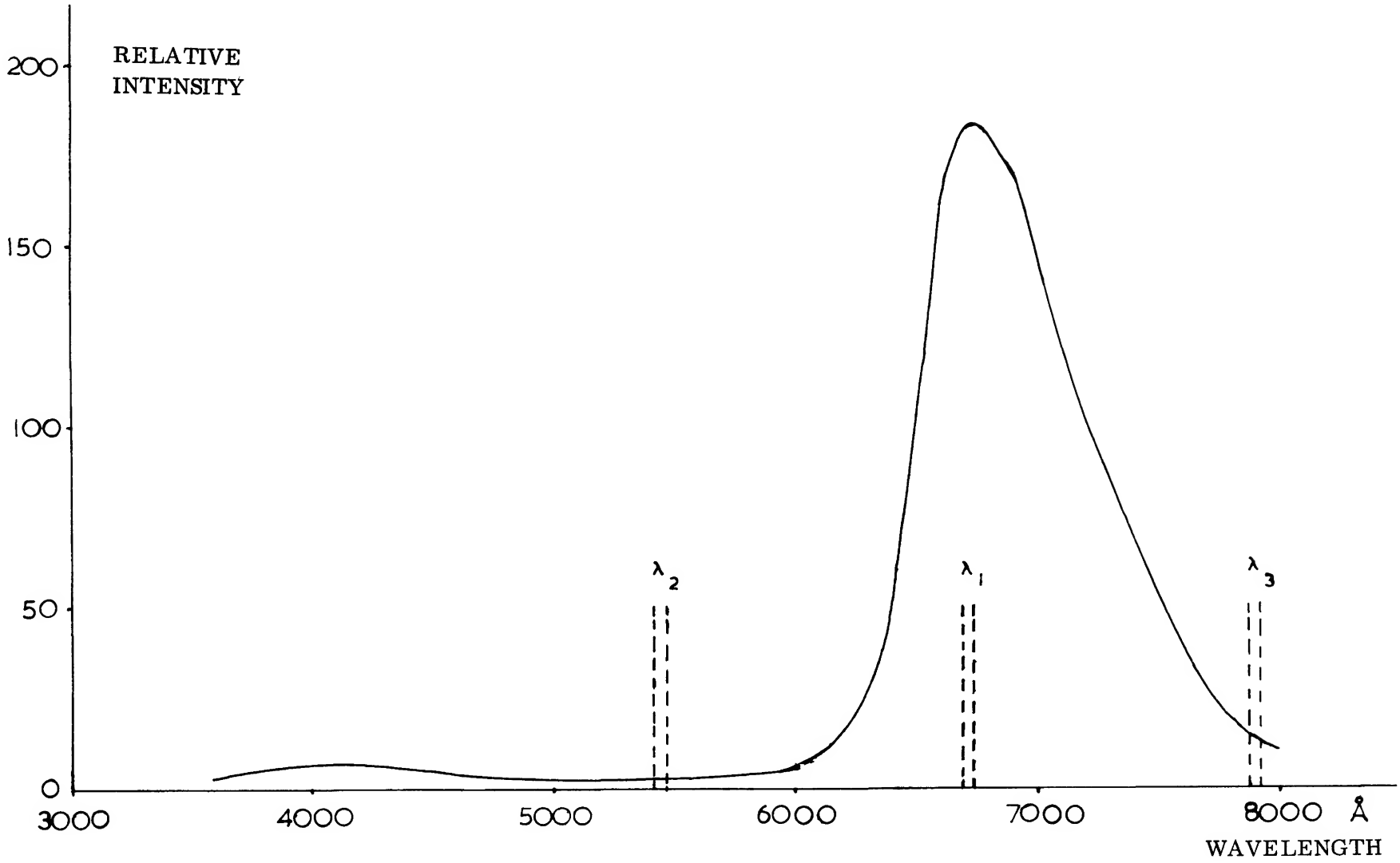

Figure 1

THE LUMINESCENCE CURVE OF THE KHOR TEMIKI METEORITE UNDER PROTON EXCITATION

(AFTER GEAKE ET AL. 1964)

Previous work (10) has shown that a change in the intensity of the stimulant changes the intensity of the luminescence but does not change the spectral profile of the luminescence band. Thus the ratio of the luminescence at a wavelength λ_1 to that at wavelength λ_2 remains constant, irrespective of intensity changes in the stimulant. Referring to Figure 1 we see that the luminescence at $\lambda 6700 \text{Å}$ is approximately one hundred times that at $\lambda 5500 \text{Å}$, thus we can say that $L_1 \sim 100 L_2$. It is also known (11) that the lunar reflectivity changes slowly with wavelength, thus we can approximate $S_1 = S_2$. Inserting these assumptions in equation 2.1 we obtain:

$$\frac{\delta R}{R} = \frac{\delta L_1}{L_1 + S_1} - \frac{\delta L_1}{L_1 + 100 S_1} \qquad 2.2$$

The value of L_1 is normally of the order of ten per cent of S_1 (3), the largest reported value at the wavelength considered ($\lambda 6700 \text{Å}$) being ninety per cent (6). In view of this, the second term on the right-hand side of equation 2.2 become negligible in comparison with the first term. Hence:

$$\frac{\delta R}{R} \sim \frac{\delta L_1}{L_1 + S_1}$$

Thus the fractional change in the ratio is effectively a direct measure of the fractional change in the luminescence. (This case no longer holds when $L_1 \sim L_2$ because the ratio is sensitive to relative changes in the intensities of the two signals.) The accuracy in the measurements of the ratio is determined by the mode of display and, if a chart recorder is used, this accuracy is of the order of one per cent.

Design Considerations

In the design of an astronomical photoelectric photometer there is a minimum of six essential components. These are (i) a finding-guiding system; (ii) a focal plane diaphragm containing at least one hole of a suitable size for isolating desired objects; (iii) a field (or Fabry) lens; (iv) suitable filters for isolating the desired spectral regions; (v) a suitable detector (including amplifier) for the radiation being measured; and (vi) a convenient method of displaying the information obtained. Additional components may increase the convenience or usefulness of the photometer.

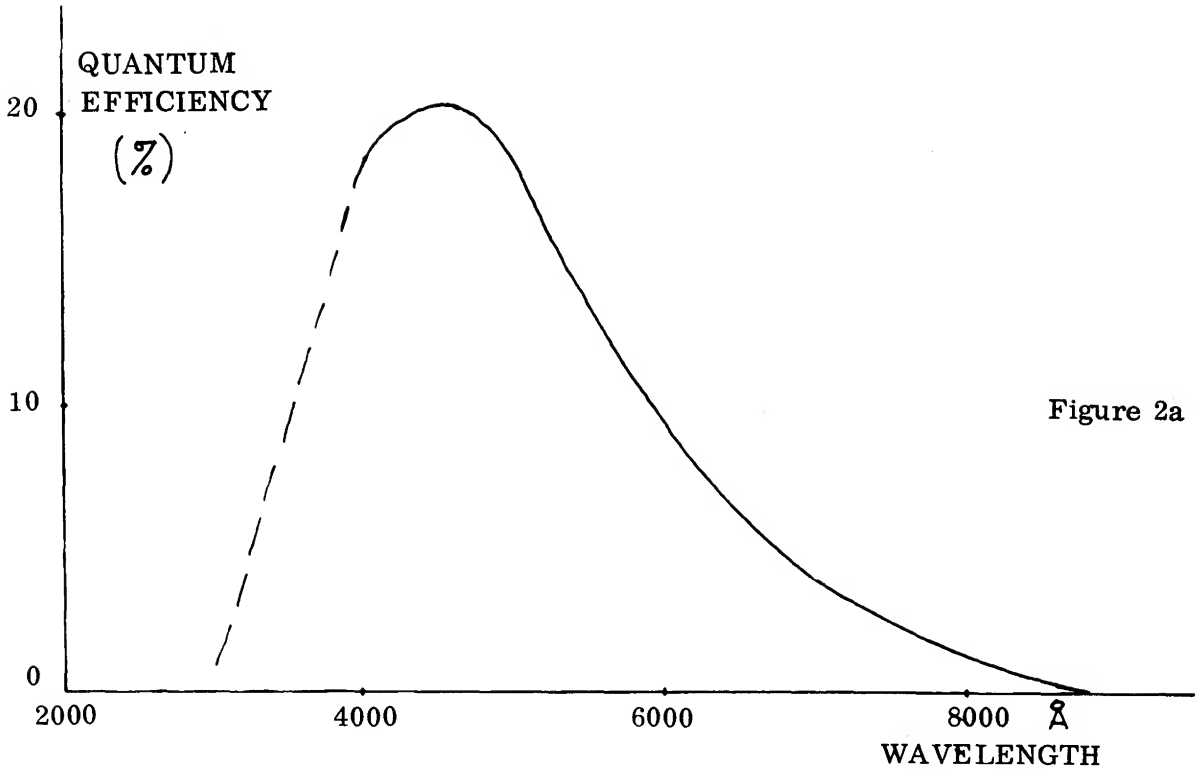

Figure 2a

SPECTRAL SENSITIVITY OF 9558B PHOTOMULTIPLIER

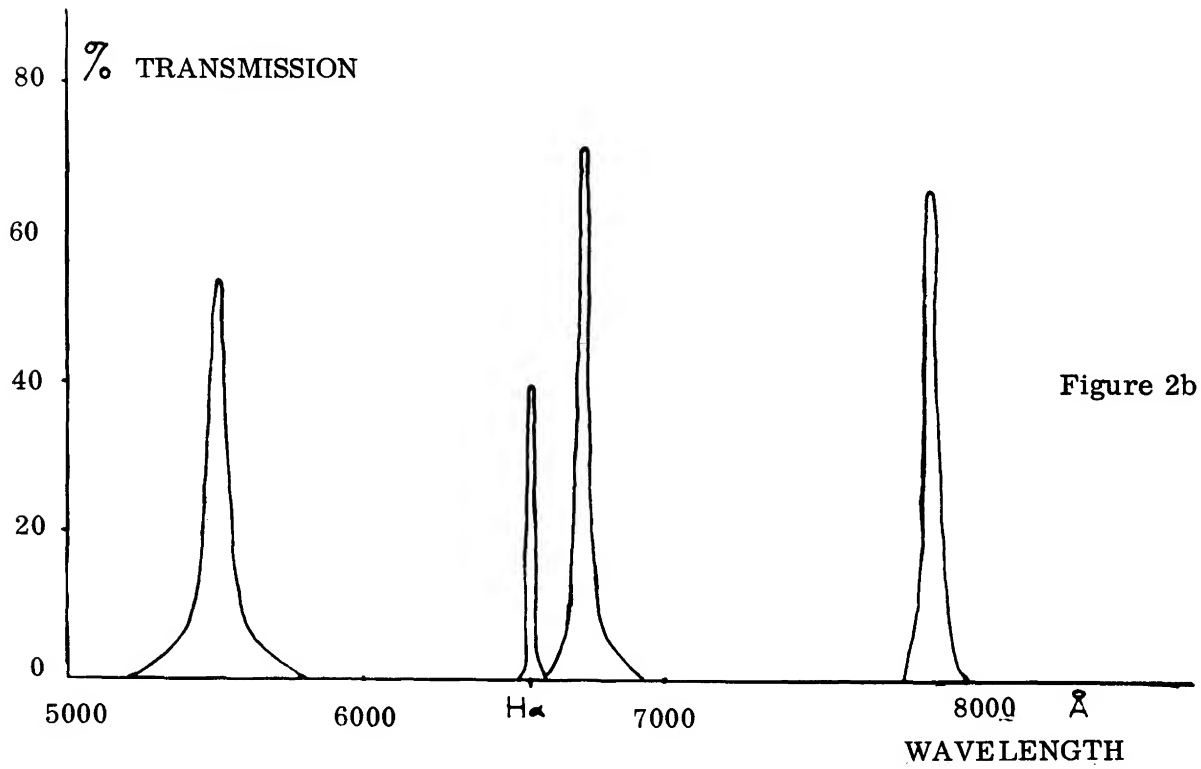

Figure 2b

FILTER TRANSMISSION CURVES

The photomultiplier to be used was chosen because of its wide spectral response (Figure 2a) and the type of electronic equipment to be used was selected on the grounds of the expected signal strength. Energy considerations showed (7) that an amplifying system which could handle currents of 2×10^{-8} amps without adding any significant noise of its own, and which had a time constant greater than 0.1 sec, was required. These requirements are met by the Avo DC Amplifier (Type 1388B), which is fitted with a 0 - 100 mV socket for use with a potentiometric pen recorder. Furthermore this amplifier has been used successfully by previous workers (4, 12) in the Department of Astronomy of the University of Manchester.

The Single Beam Photoelectric Photometer

The single beam photoelectric photometer, illustrated in Figure 3 and 4, was designed for use with either the side window blue-sensitive E.M.I. 9661B photomultiplier or with the end window trialkali tube E.M.I. 9558B. For the luminescence work the 9558B photomultiplier was used due to its wide spectral response shown in Figure 2a.

Guidance was effected by means of a mylar film stretched at 45° to

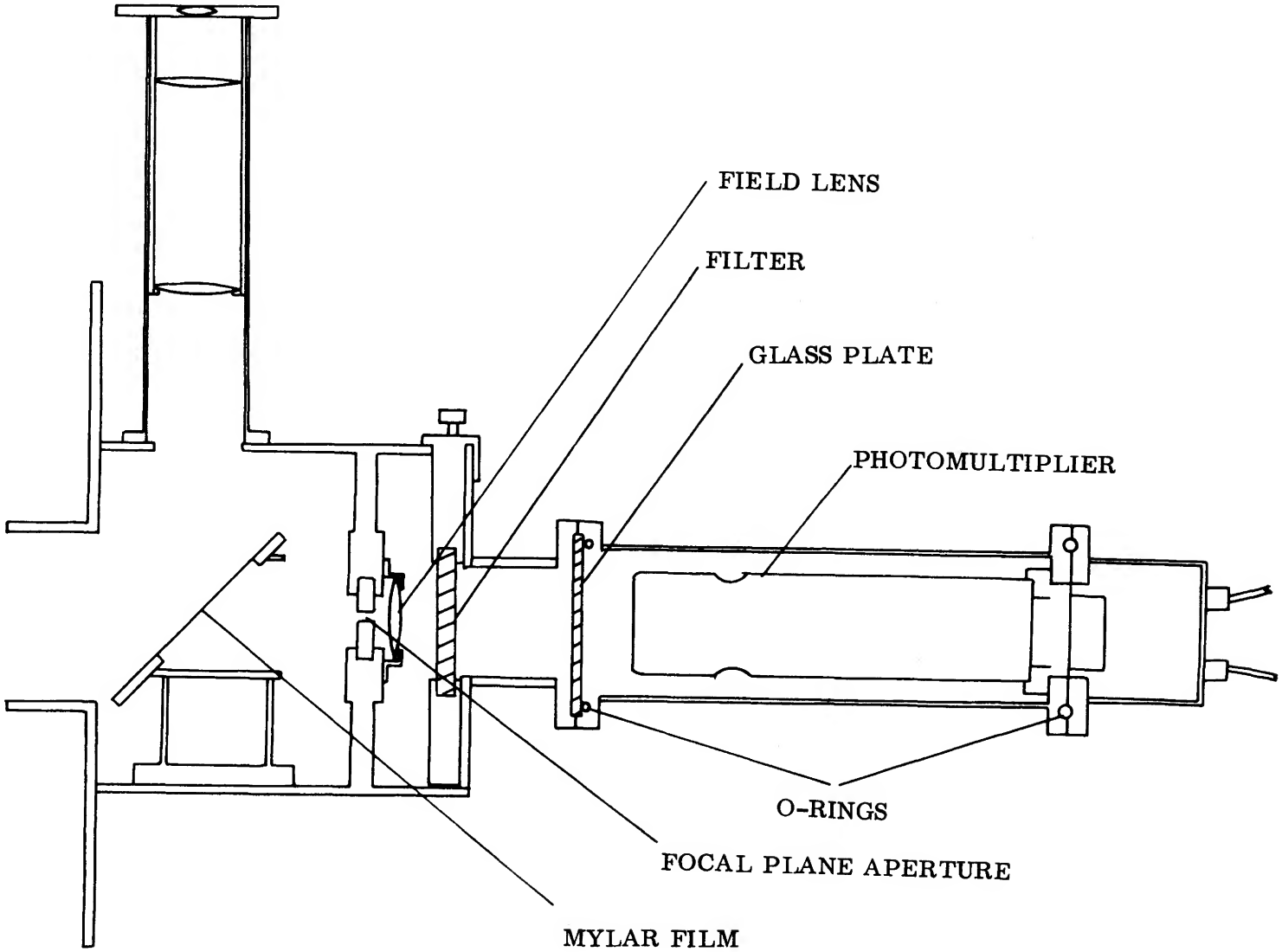

Figure 3

THE SINGLE BEAM PHOTOMETER

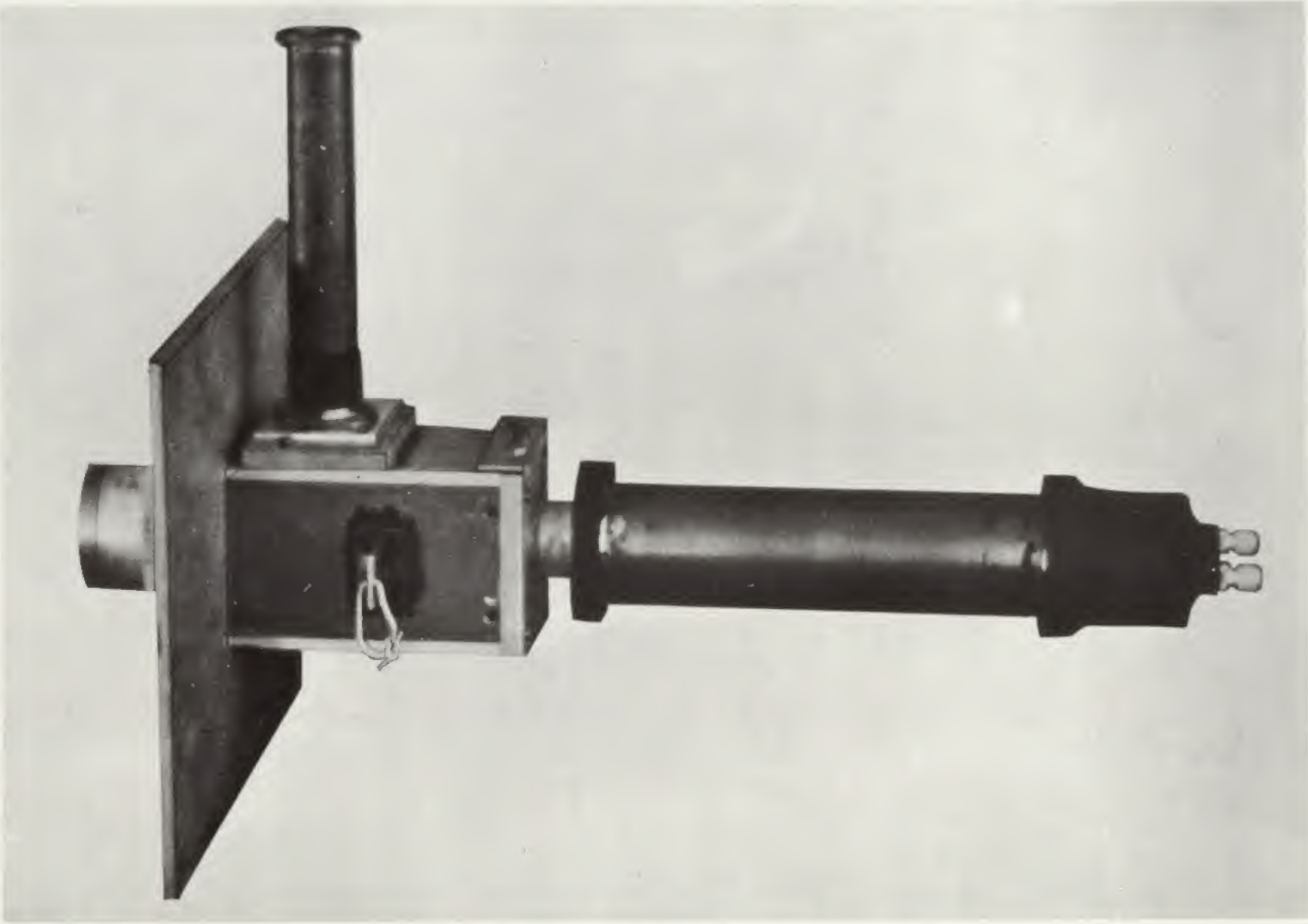

Figure 4

THE SINGLE BEAM PHOTOELECTRIC PHOTOMETER

the optical axis and a viewing tube at right angles to the optical axis. The object for analysis could thus be centred and viewed for the duration of an experiment. The magnification of the viewing system was five.

The focal plane aperture consisted of a hole drilled in a rectangular metal slide which was pushed into position through an opening in the side of the photometer and accurately located by means of a spring. Several of these slides were made with holes varying from 0.1 mm. to 2.0 mm., corresponding approximately to 1 and 20 seconds of arc. The size of the focal plane aperture could thus be changed merely by changing the slides.

The field lens, immediately behind the focal plane aperture, had a focal length of 14 cm. and imaged the telescope objective on the photocathode of the photomultiplier. The filters were held in slides which pushed into position through an opening in the top of the photometer. The transmission curves of the filters used are shown in Figure 2b. The photomultiplier was kept free of moisture by silica gel crystals held in a plastic container in the resistor housing.

The dynode chain of the photomultiplier (E.M.I. Type 9558B) was

fed by an Isotopes Development stabilized high tension power pack (I.D.L. 532D) with a range of 500 to 3000volts. The output from the multiplier was fed directly to an Avo DC amplifier Type 1388B. The current range of the instrument is from 10^{-6} to 3×10^{-13} amps for full scale meter deflection, and there is a switch which provides seven imput ranges. An output of 100 mV at full scale deflection is provided to operate a chart recorder. This output was displayed on a Honeywell Chart Recorder which required 100 mV for full scale deflection.

The single beam photometer and the associated electronic equipment were shipped to France in the summer of 1963. Preliminary work on luminescence started with this instrument in November 1963, but prior to this, some experiments were carried out in the laboratory.

Laboratory Experiments

Experiments were carried out to test the effect of the Earth's magnetic field on the gain of the photomultiplier and also to test the effect of changing the applied voltage on the signal-to-noise ratio of the photomultiplier. The magnetic field experiments were carried out in greater detail with the three-

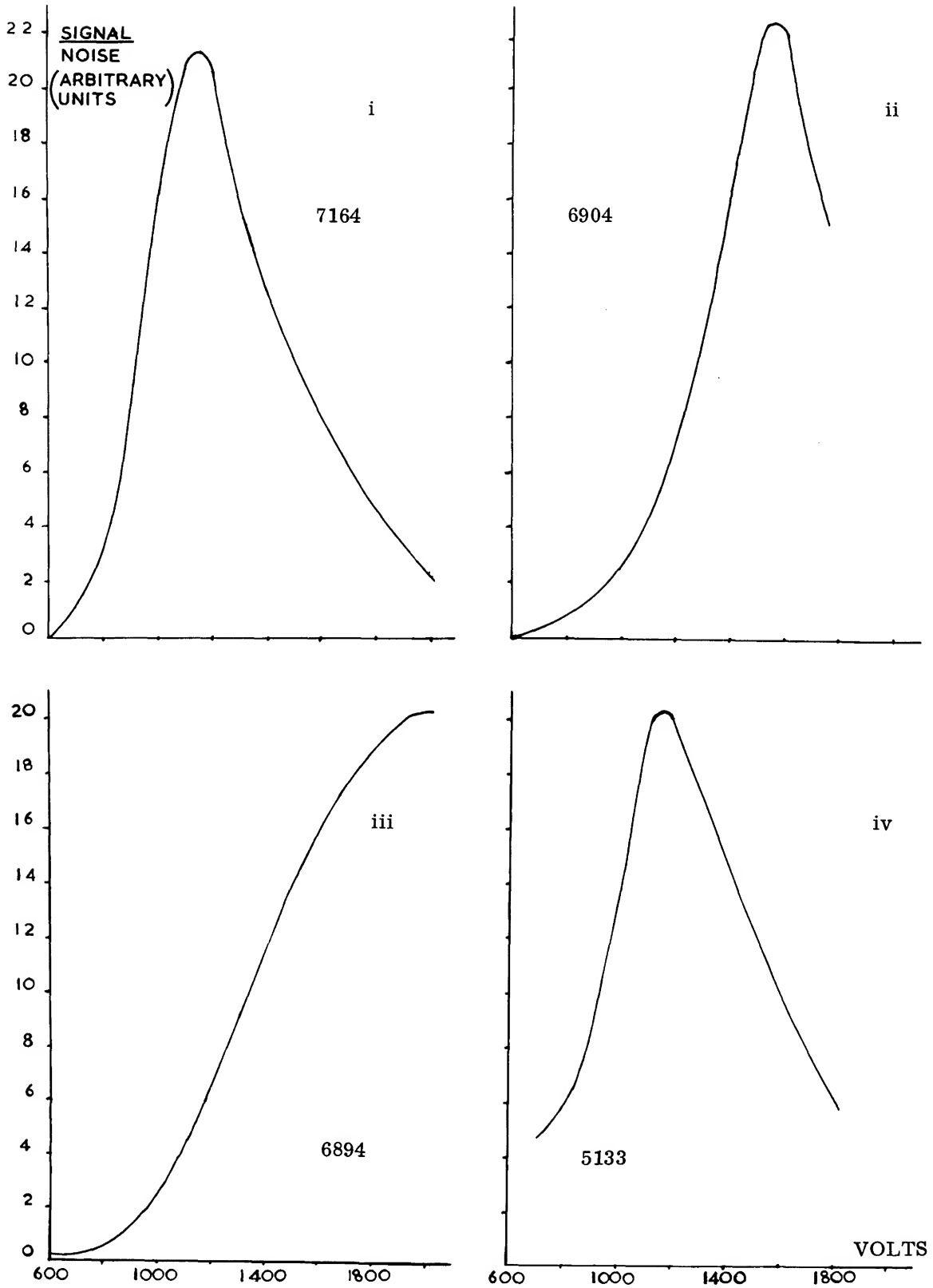

Figure 5

EFFECT OF VOLTAGE ON SIGNAL TO NOISE RATIO OF 9558B PHOTOMULTIPLIERS

beam instrument and will, therefore, be described in the next section.

In view of conflicting statements (13, 14) about the behaviour of photomultipliers with increasing applied voltage it was decided to measure the effect of changing the applied overall voltage on the signal-to-noise ratio of a photomultiplier, in order to find the optimum working voltage. The voltage was changed in steps of 100 volts from 600 to 2000 volts using the voltage adjuster on the H.T. set, and the dark current was read off on the chart recorder. Using a stabilized neon lamp as a light source this process was repeated. When more photomultipliers of the same type (9558B) were available this experiment was repeated and the combined results are shown graphically in Figure 5.

It can be seen that the signal-to-noise ratio rises to a maximum with increasing voltage and in three cases, falls as the voltage is increased further. In the fourth case there is evidence of peak at 2000 volts. The interesting point is that the four photomultipliers have the best signal-to-noise ratio at different voltages even though all tubes are of the same type (9558B). In view of the above, the operating voltage for the multiplier used with the single beam photometer (Serial No. 5133) was chosen as 1150 volts (Figure 5iv).

Observations at the Telescope

The first observations at the telescope were made on the night of 30th November, 1963 when the Moon was fourteen days old. This was the lunation immediately following the one during which Kopal and Rackham (6) photographed the transient red enhancement of the Kepler area. It was intended to see if any enhancement was also visible during this full Moon. The method of observation was to take a reading, say on Copernicus, with one filter, then take another reading, say on Kepler, with the same filter as quickly as possible. This process was then repeated several times. After several readings the filter was changed and the whole process repeated. In this way it was hoped to monitor any transient relative phenomenon involving Copernicus and Kepler, which had been observed during the previous full Moon. The results for the night 30th November, 1963 are gathered in Table 2.1 and although the scatter of these results is high there is certainly no transient luminescent effect of the same magnitude as reported on 2nd November, 1963.

By taking the ratio of the Copernicus to Kepler readings it was hoped to

average out general atmospheric transparency changes.

The 'range' and 'scale' referred to in Columns 2 and 3 are the range and scale of the Avo DC Amplifier, thus a reading of 28.5 on the 10^4 range, -10 scale corresponds to a current from the photomultiplier of 2.85×10^{-8} amp.

Taking the ratio of the Copernicus to Kepler readings would also eliminate any change in gain of the photomultiplier with orientation relative to the Earth's magnetic field.

The scatter of the Copernicus to Kepler ratios is large in all colours due in part to the weather conditions causing transparency fluctuations. It would be difficult to attribute these fluctuations to luminescence. Under these conditions the luminescent intensity would have to change by at least 10% of the scattered sunlight, and even in ideal observing conditions it would be difficult to detect 5% changes due to luminescence using a single beam photometer. Tables 2.2, 2.3 and 2.4 show the results obtained on subsequent nights. The decrease in the Copernicus to Kepler ratio in all colours over a period of a week is just a manifestation of the relative angle of elevation of the Sun for the two regions.

TABLE 2.1

Date: 30.11.63
1.12.63

Time	Range	Scale	Copernicus	Kepler	Copernicus / Kepler	Filter	Comments
23.45	10^5	-10	51.0	39.5	1.29	Green	Occasional cloud
23.46	10^5	-10	53.0	41.5	1.28	Green	interrupting readings
23.47	10^5	-10	53.0	40.0	1.33	Green	
23.49	10^5	-10	56.0	40.0	1.40	Green	
23.50	10^5	-10	56.0	44.5	1.26	Green	
23.51	10^5	-10	72.0	59.0	1.12	Green	
23.52	10^5	-10	72.0	61.0	1.22		
23.55	10^5	-3	65.5	50.0	1.31	Red	Occasional cloud
23.56	10^5	-3	65.5	57.0	1.15	Red	
23.58	10^5	-3	64.0	52.5	1.22	Red	
23.59	10^5	-3	63.5	52.5	1.21	Red	

TABLE 2.1 (Cont'd.)

Time	Range	Scale	Copernicus	Kepler	$\frac{\text{Copernicus}}{\text{Kepler}}$	Filter	Comments
00.00	10^5	-3	63.5	57.5	1.10	Red	
00.02	10^5	-3	65.0	57.5	1.13	Red	
00.03	10^5	-3	65.0	57.5	1.13	Red	
00.05	10^5	-3	65.0	51.5	1.26	Red	
00.07	10^5	-3	65.0	51.5	1.26	Red	
00.08	10^5	-3	65.0	50.5	1.29	Red	
00.10	10^5	-3	68.5	50.5	1.35	Red	
00.26	10^4	-10	28.5	22.5	1.27	Hα	
00.28	10^4	-3	95.0	78.0	1.22	Hα	
00.29	10^4	-3	95.0	78.0	1.22	Hα	
00.30	10^4	-3	95.0	78.5	1.21	Hα	

TABLE 2.1 (Cont'd.)

Time	Range	Scale	Copernicus	Kepler	Copernicus / Kepler	Filter	Comments
00.32	10^4	-3	98.0	78.5	1.25	Hα	
00.33	10^4	-3	98.0	77.5	1.26	Hα	
00.34	10^4	-3	95.0	77.5	1.23	Hα	
00.35	10^4	-3	95.0	81.0	1.17	Hα	
00.36	10^4	-3	94.5	81.0	1.17	Hα	
00.37	10^4	-3	99.9	94.0	1.16	Hα	
00.38	10^4	-3	99.9	82.5	1.21	Hα	
00.39	10^4	-3	98.0	82.5	1.19	Hα	
00.40	10^4	-3	98.0	78.5	1.25	Hα	
00.41	10^4	-3	82.5	78.5	1.05	Hα	

TABLE 2.2

Date: 4.12.63

Time	Range	Scale	Copernicus	Kepler	$\frac{\text{Copernicus}}{\text{Kepler}}$	Filter	Comments
00.39	10^5	-10	28.5	23.5	1.21	Green	Occasional cloud
01.28	10^5	-3	99.5	76.5	1.30	Green	otherwise clear
01.52	10^5	-10	29.5	22.0	1.34	Green	
02.21	10^5	-10	27.0	22.5	1.20	Green	
00.41	10^4	-10	93.5	68.0	1.38	Red	Different sized
01.24	10^4	-10	81.0	60.0	1.34	Red	pin-holes used
01.57	10^4	-10	70.5	63.5	1.11	Red	
02.16	10^5	-3	26.0	20.0	1.30	Red	
00.45	10^3	-10	30.5	22.0	1.38	I.R.	Different sized
01.15	10^3	-3	99.0	73.5	1.34	I.R.	pin-holes used
02.02	10^3	-3	78.0	65.0	1.20	I.R.	
02.12	10^3	-3	82.5	62.0	1.33	I.R.	

TABLE 2.2 (Cont'd.)

Time	Range	Scale	Copernicus	Kepler	Copernicus / Kepler	Filter	Comments
00.51	10^4	-3	52.0	40.0	1.30	Hα	
01.12	10^4	-3	53.0	40.0	1.32	Hα	
01.53	10^4	-3	43.0	34.0	1.27	Hα	
02.19	10^4	-3	42.0	33.0	1.27	Hα	

TABLE 2.3

Date: 5.12.63

Time	Range	Scale	Copernicus	Kepler	$\frac{\text{Copernicus}}{\text{Kepler}}$	Filter	Comments
00.16	10^3	-3	67.0	58.0	1.22	I.R	Cloud occasionally
00.25	10^4	-10	47.0	41.0	1.15	Red	prevented readings
00.33	10^3	-10	66.0	65.0	1.01	Hα	
00.46	10^5	-3	54.0	45.0	1.20	Green	

TABLE 2.4

Date: 6.12.63

Time	Range	Scale	Copernicus	Kepler	$\frac{\text{Copernicus}}{\text{Kepler}}$	Filter	Comments
01.15	10^3	-3	34.0	54.0	0.63	I.R.	Weather clear
04.16	10^2	-10	27.0	40.0	0.68	I.R	
01.23	10^4	-10	37.0	60.0	0.62	Red	
04.08	10^4	-3	32.0	50.0	0.64	Red	
01.30	10^3	-10	54.0	85.0	0.64	Hα	
04.03	10^3	-3	47.0	75.0	0.63	Hα	
01.35	10^5	-3	40.0	65.0	0.62	Green	
03.53	10^4	-10	31.0	50.0	0.62	Green	

It is evident from the above results that a system of compensating for atmospheric and guidance effects must be used if small changes in the luminescence are to be detected.

An instrument which incorporates such a compensating system is described in the next section.

SECTION III

THE THREE BEAM PHOTOELECTRIC PHOTOMETER

An instrument designed to measure the light from an astronomical object in three wavebands simultaneously is described in this section. Experiments on the change in gain of photomultipliers with orientation are described. The results obtained at the telescope are collected in the next section. The three beam instrument was designed for use with either the 43-inch f/15 reflector or the 24-inch f/30 refractor at the Pic-du-Midi Observatory in France. Up to the present time, however, all the observing work has been carried out with the 24-inch refractor.

The three beam instrument is illustrated schematically in Figure 6 and photographically in Figures 7 and 12. A few per cent of the light beam entering the photometer is deflected into the first guidance system. The beam then passes through the iris diaphragm aperture and a further portion of the light is deflected from the main beam for a second guidance system. The collimating lens presents a parallel beam of light to the beam splitters and filters, and the field lenses image the telescope objective on

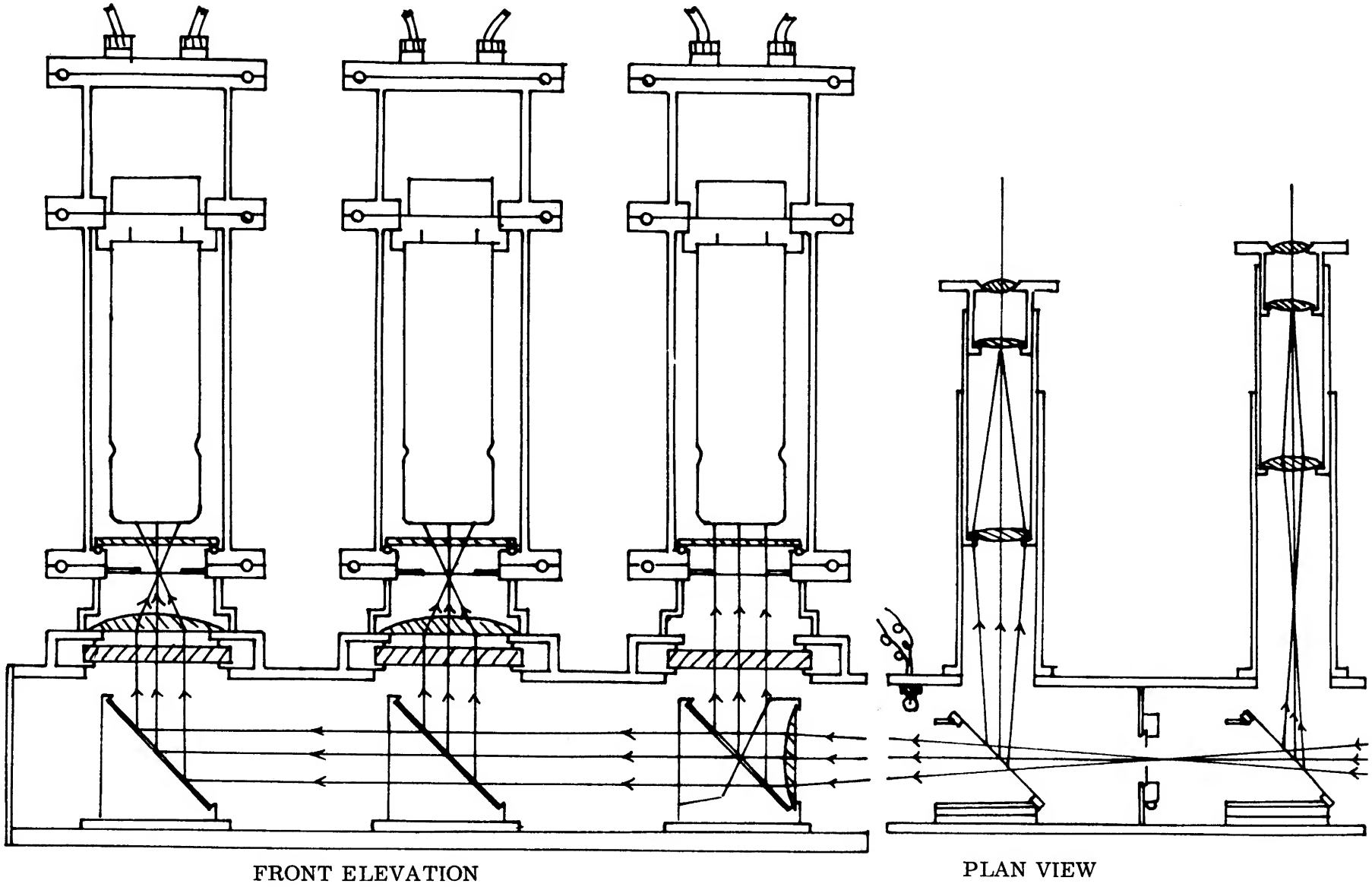

Figure 6

THE THREE BEAM PHOTOELECTRIC PHOTOMETER

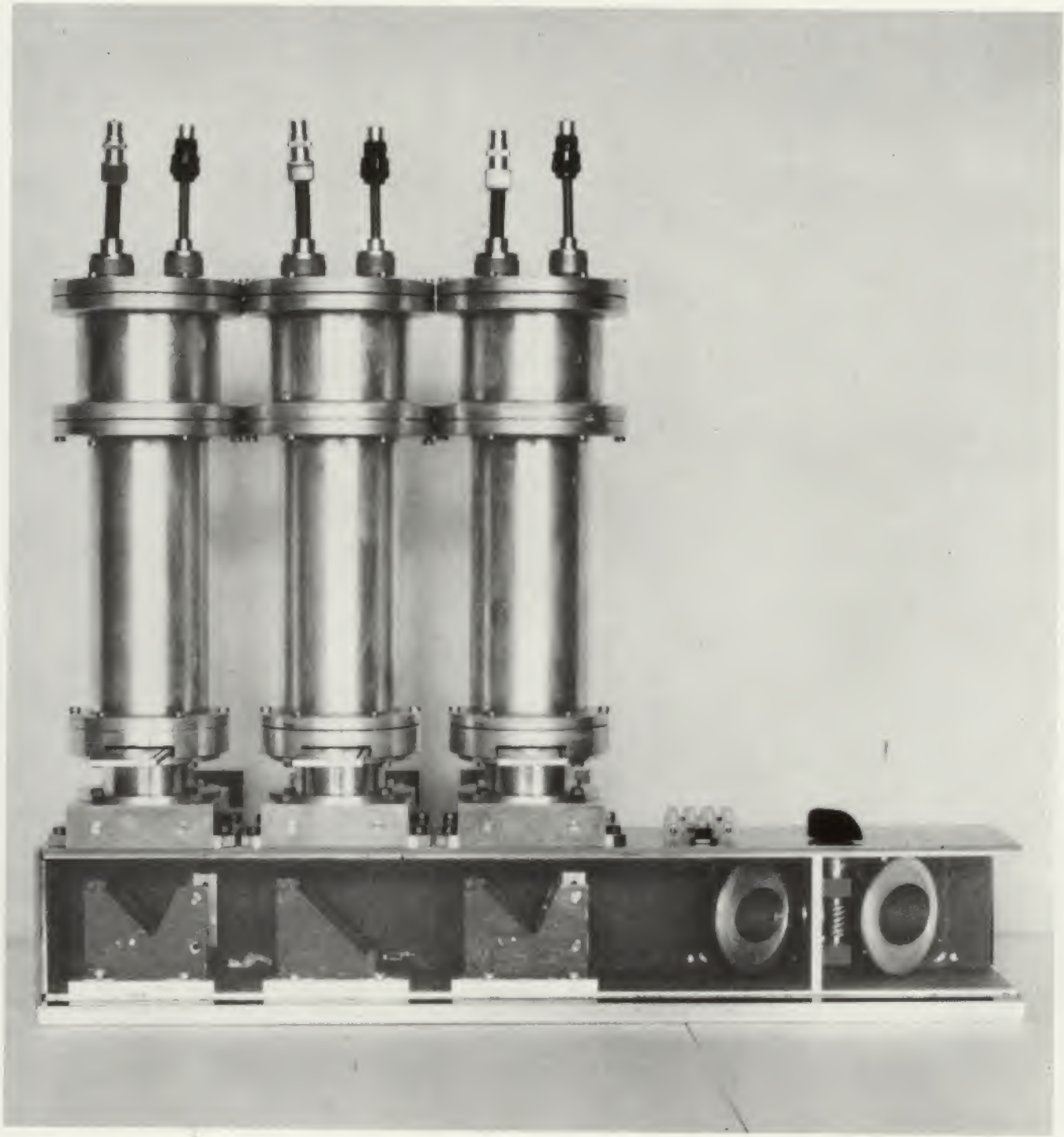

Figure 7

THE THREE BEAM PHOTOMETER WITH SIDE REMOVED

the photocathodes of the respective photomultipliers.

The field of view of the first guidance system when used with the f/30 refractor is about five minutes of arc and the magnification is two. Double images are prevented by the use of mylar film (thickness $\sim \frac{1}{1000}$ inch) which also has the advantage of not colouring the transmitted light (Figure 8). The mylar film holders can be seen in position in Figure 7.

The size of the iris diaphragm aperture can be altered by turning a pointer (attached by a worm wheel drive to the iris diaphragm) on the upper side of the photometer. The aperture range is 0.6 to 0.8 mm, corresponding respectively to five and seventy seconds of arc in the focal plane of the f/30 refractor.

Partially aluminised beam-splitters, in preference to partially silvered or all dielectric beam-splitters, were chosen as these permitted a more versatile instrument (7). Silver has the disadvantage that it absorbs light strongly below $\lambda 4000 \text{Å}$ (Figure 9a), and for all dielectric beam-splitters the ratio of reflectivity to transmissivity changes appreciably with the wavelength of the incident light. The absorption of light by aluminium (Figure 9b)

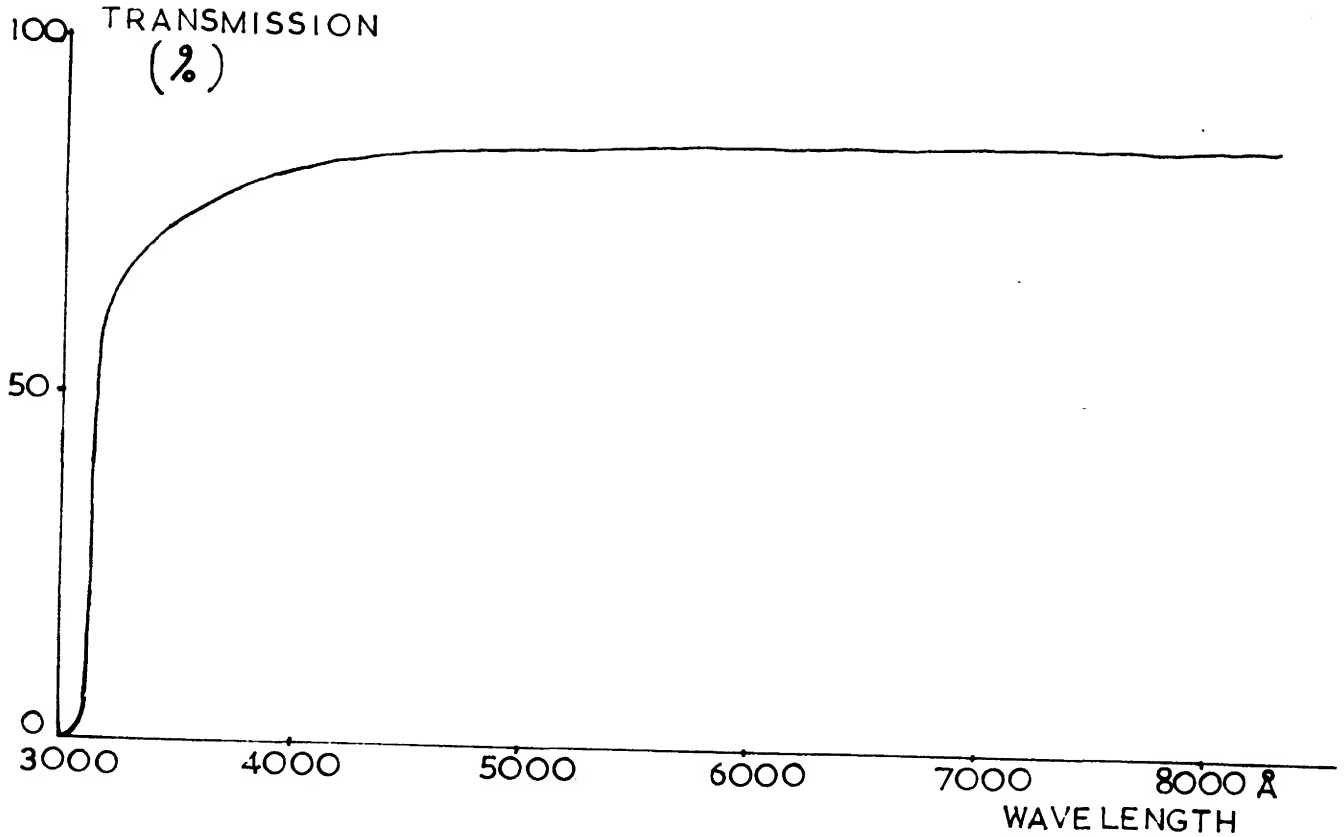

Figure 8

CURVE OF TRANSMISSION VERSUS WAVELENGTH FOR MYLAR

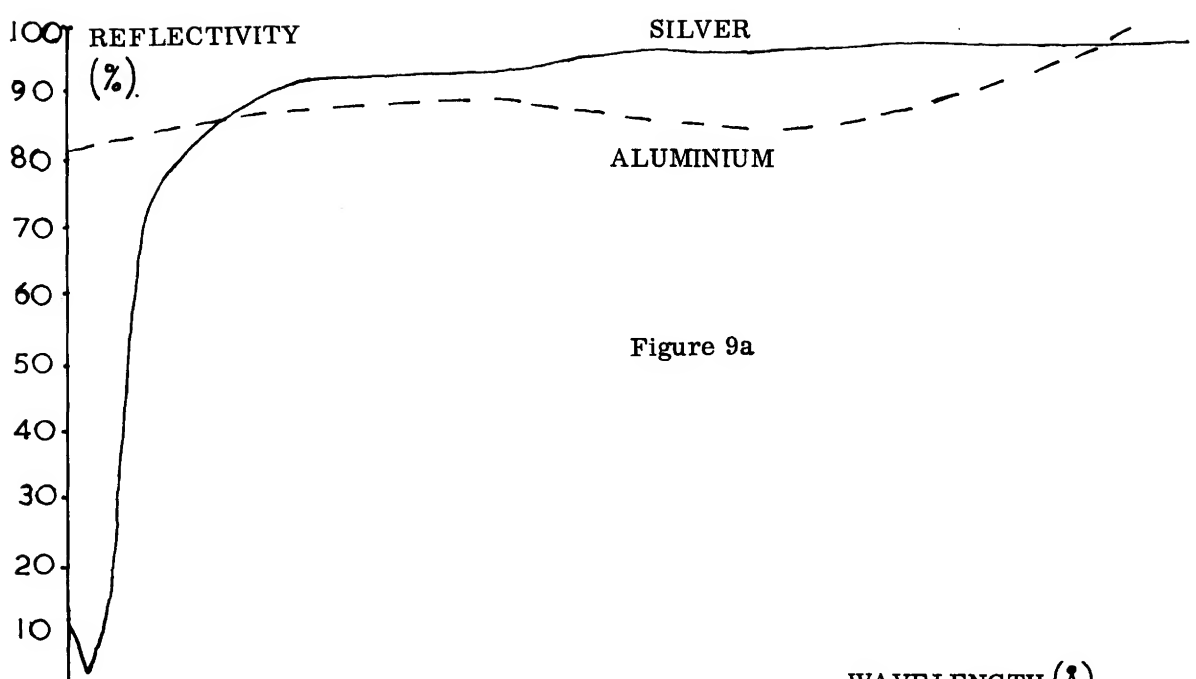

Figure 9a

REFLECTIVITY OF SILVER AND ALUMINIUM SURFACES

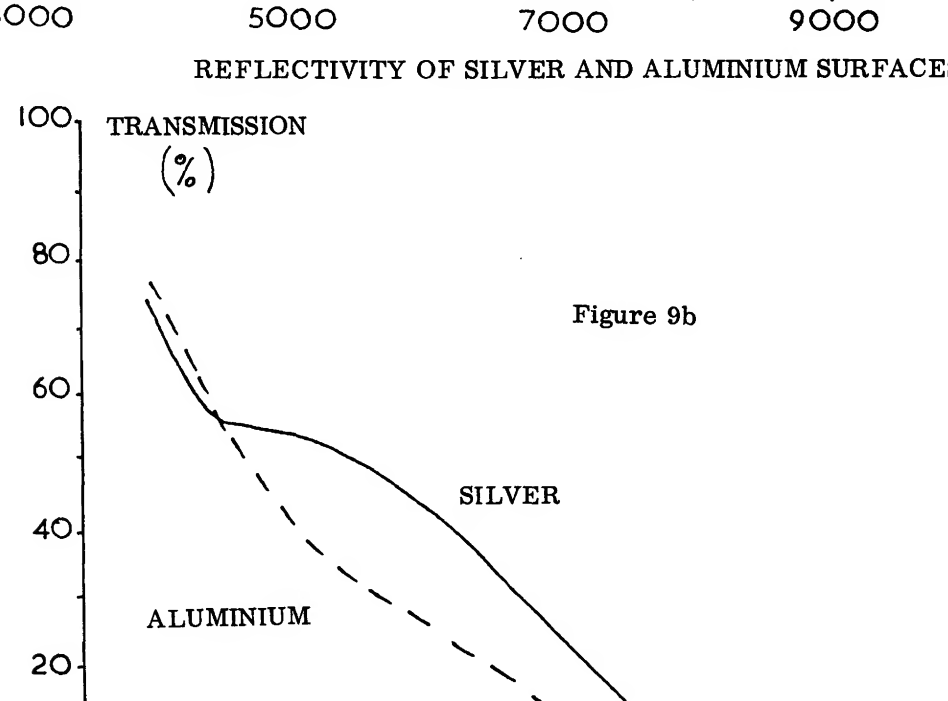

Figure 9b

REFLECTION AND TRANSMISSION OF PARTIALLY REFLECTING SURFACES

however, necessitates the calculation of the required ratio of transmissivity to reflectivity for the respective beam-splitters such that the light is split up into three equal components. This calculation shows (7) that the reflectivity of the first beam-splitter should be 20% and the transmissivity should be 55%, the corresponding figures for the second beam-splitter being 36% and 39%, respectively; assuming an absorption of 25% for the partially aluminised beam-splitters (Figure 9b), and 10% for the fully aluminised beam-splitters.

The transmission - reflection curves of the beam-splitters used is shown in Figure 10. Though not entirely to specification (due to manufacturing difficulties with protective and anti-reflecting coatings) this is not serious in the case of the Moon as plenty of light is available. The beam-splitter supports can be seen in position in Figure 7. The beam-splitters in addition to the filters (Figure 2b) were manufactured by Sir Howard Grubb Parsons and Co. Ltd.

The filter holders, field lens holders and photomultiplier housings make up the units which screw into position on the upper side of the main box of the photometer (Figures 6 and 7). Light from the telescope enters the air-tight housings through a plate glass window. The air inside the housings is kept

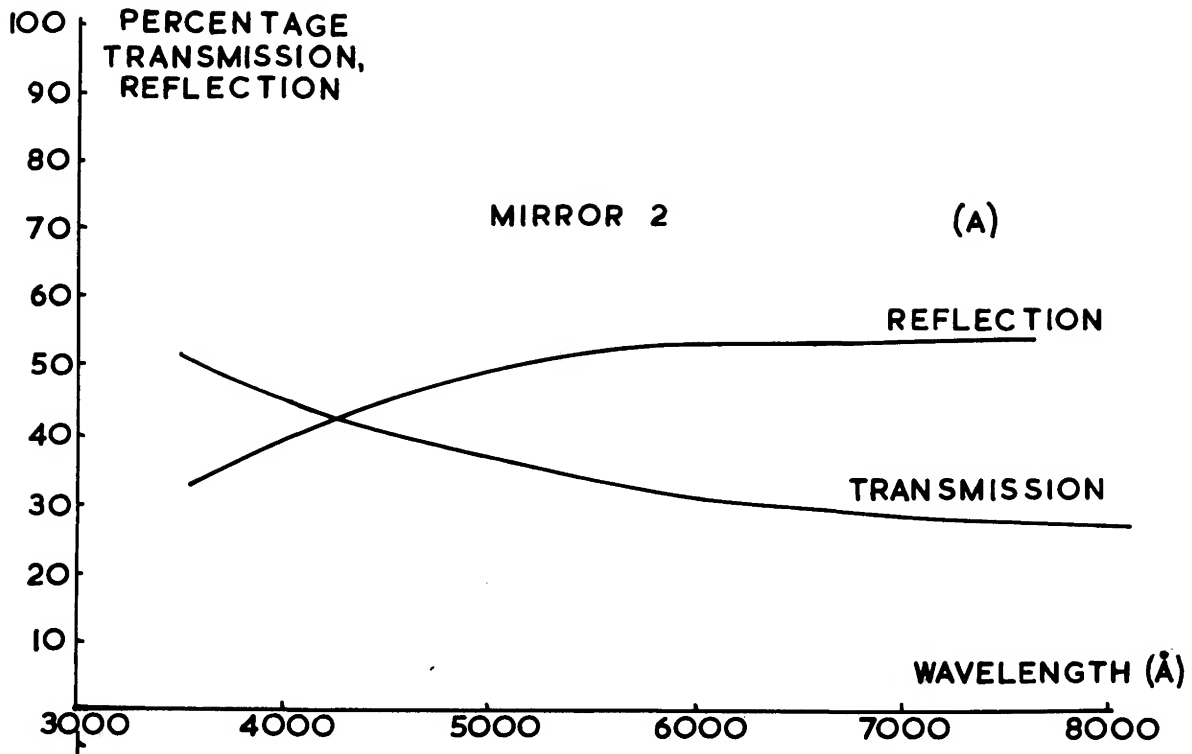

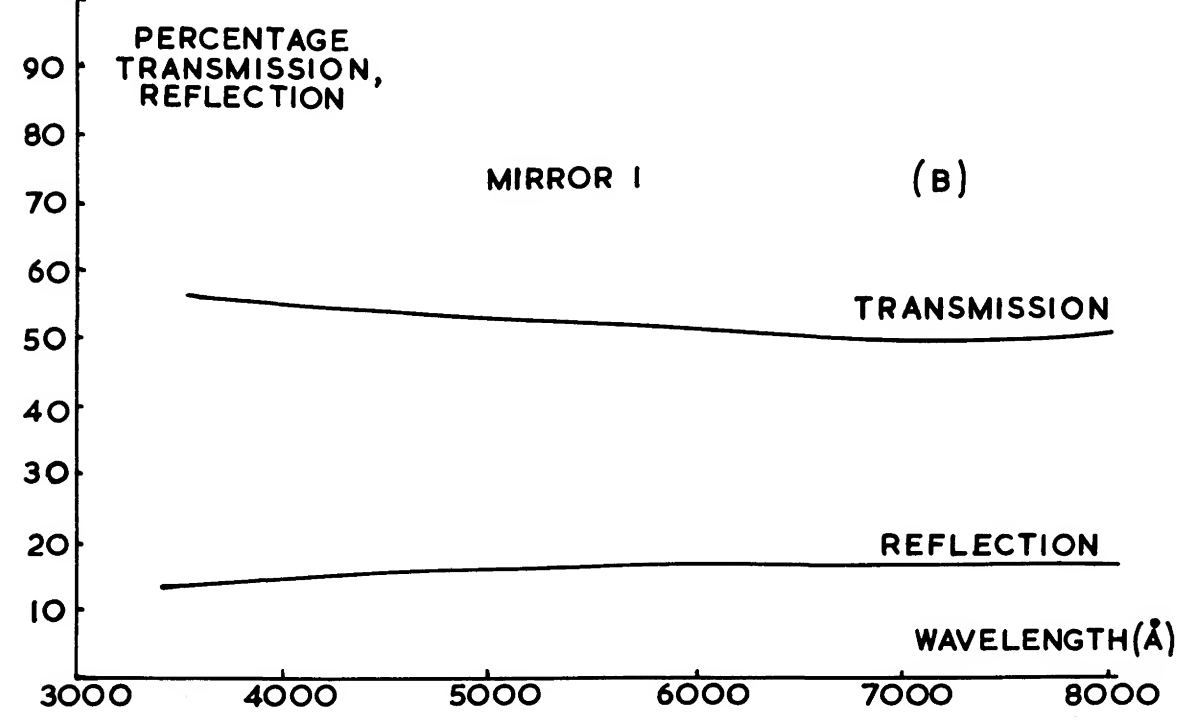

Figure 10

CURVES OF TRANSMISSION AND REFLECTION VERSUS WAVELENGTH FOR THE PARTIALLY ALUMINISED BEAM SPLITTERS

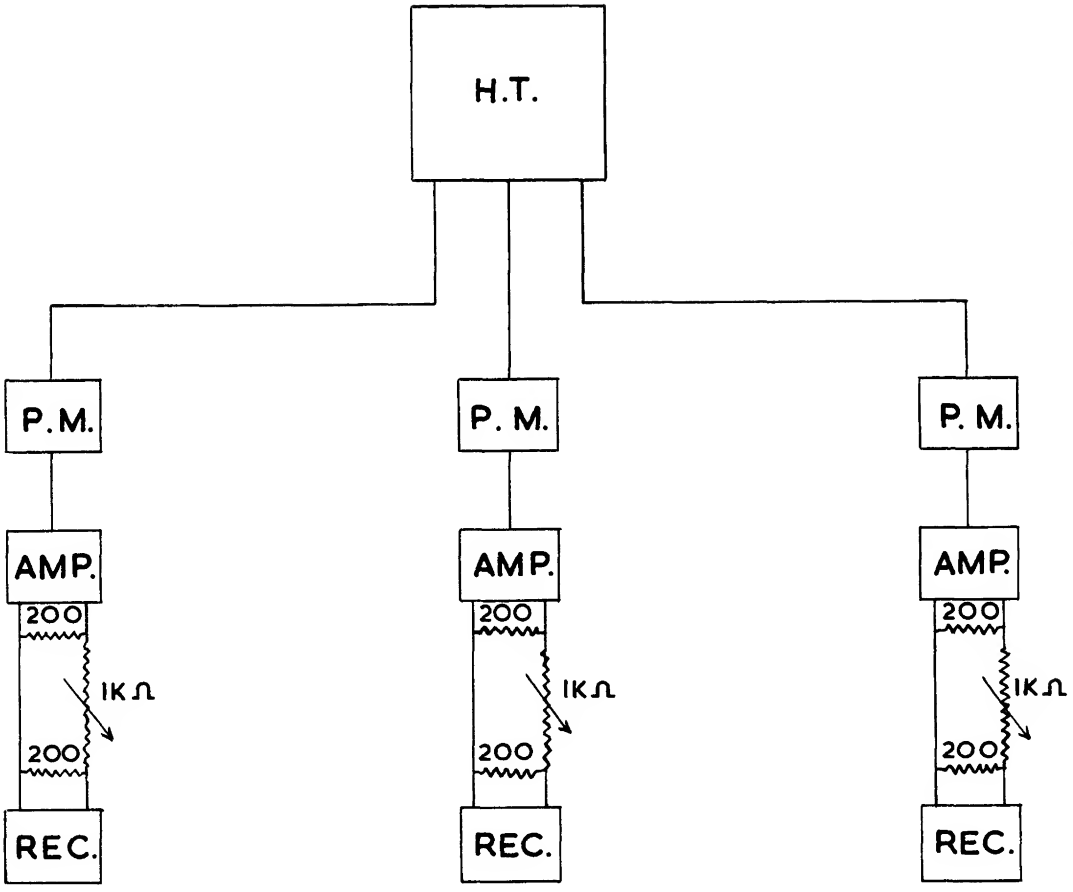

Figure 11

BLOCK DRAWING OF MEASURING SYSTEM

moisture free with silica gel crystals. The housings are designed for use with E.M.I. 9558B photomultipliers and the spectral response of this type of multiplier is shown in Figure 2a .

Basically the same electronic system was used as with the single beam photometer, except that in this case there were three signals to amplify. The same high tension supply (Type I.D.L. 532D) was used for all three photomultipliers and the anode current of each photomultiplier was amplified by an Avo D.C. Amplifier, Type 1388B . The amplified signals were displayed on three chart recorders which had the same time response and full scale deflection. Double shielded "Aquadag" (B.I.C.C. Ltd.) co-axial cable was used for the signal cables and a system was incorporated whereby a given signal could be placed on any part of the recorder scale. A switch enabled the three pen recorders to be started simultaneously. A block drawing of the measuring system is shown in Figure 11 .

The photometer on its telescope mounting is shown in Figure 12 . This mounting allows five inches of movement along the optical axis thus permitting accurate focusing.

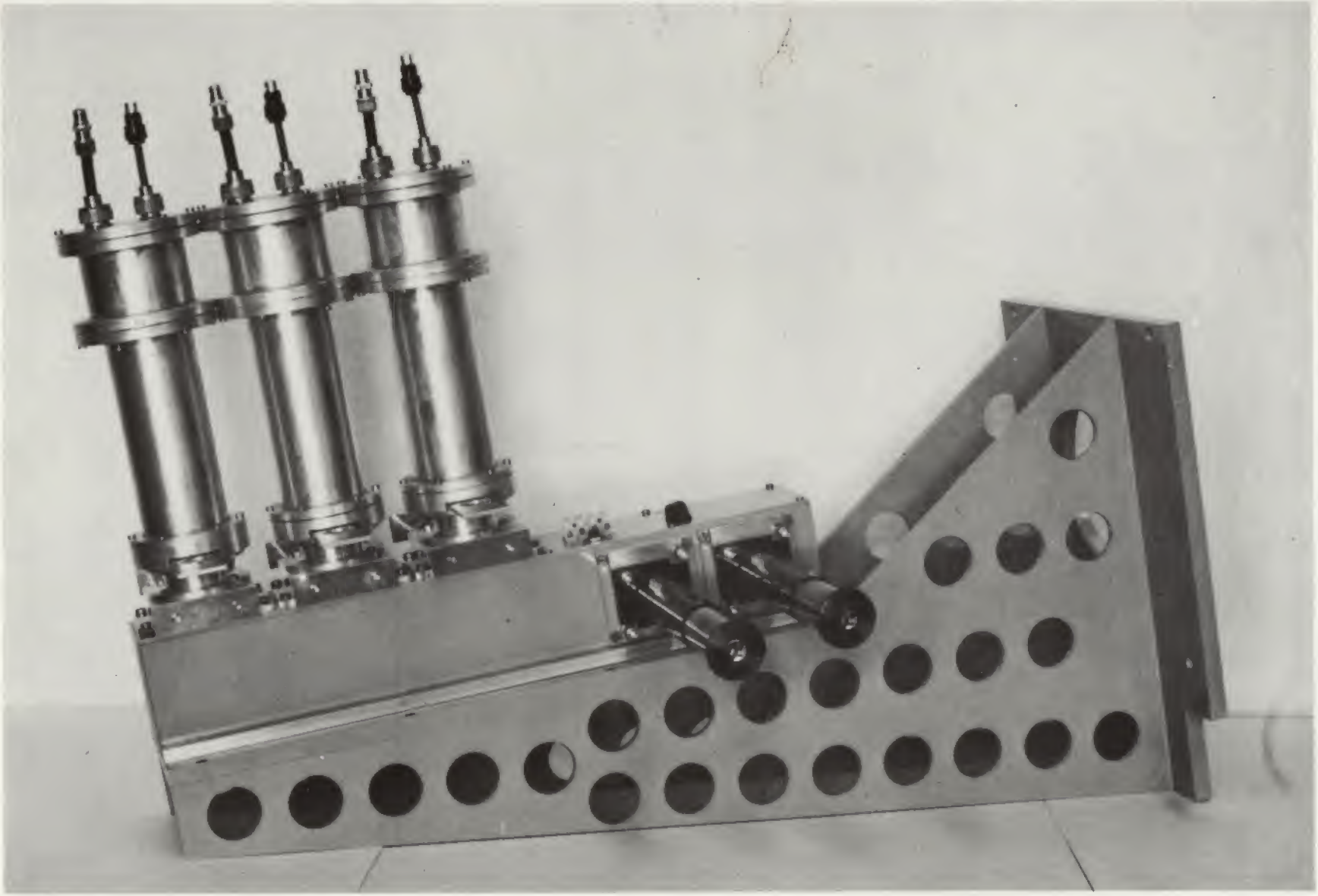

Figure 12

THE THREE BEAM PHOTOMETER ON ITS TELESCOPE MOUNTING

Laboratory Experiments

Before the instrument was used to study the Moon, experiments were carried out to test the effect of the Earth's and stray magnetic fields on the gain of the photomultipliers.

It is known (14) that the presence of a magnetic field can deflect electrons which travel through an electron multiplier causing them to miss a dynode surface. Experiments on the change in gain of a photomultiplier with orientation relative to the Earth's magnetic field have been carried out by Eggen (15), and more recently by Clarke (12) who used E.M.I. photomultipliers. Clarke showed that mu-metal screening considerably reduced the deviations in the signal produced by the magnetic field, but even with screening his curves still show a two per cent change in signal when the multiplier is rotated through 180°.

Experiments were therefore carried out using a stabilised neon lamp, fitted to the front of the photometer, as a light source. The photometer was attached to the telescope and the signals from the three photomultipliers, for different orientations of the telescope, were measured on the chart recorders.

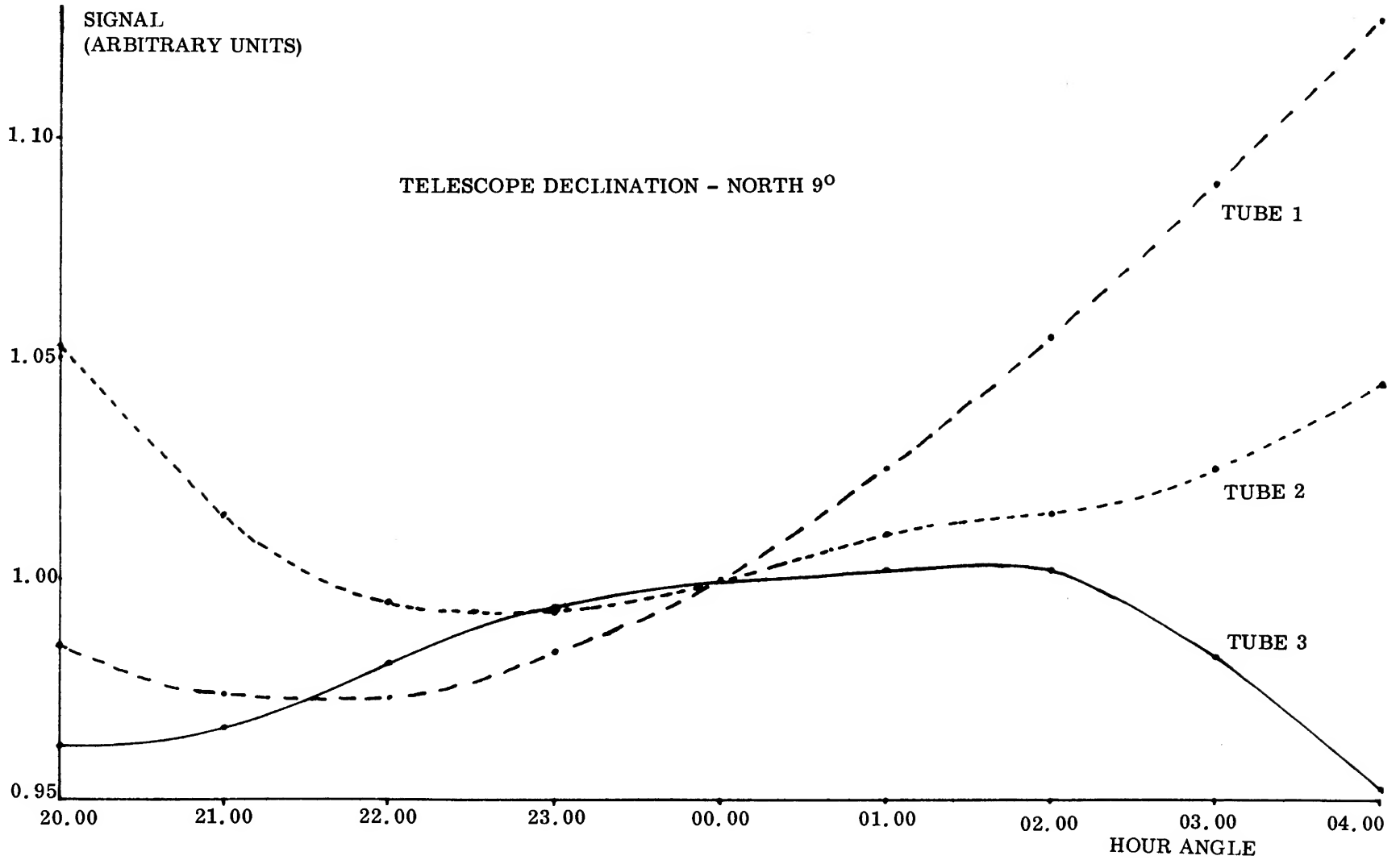

Figure 13

THE EFFECT OF THE TELESCOPE ORIENTATION ON THE PHOTOMULTIPLIER SIGNALS

Figure 13 shows the changes in the signals for different telescope orientations. The signals from the three photomultipliers changed independently of one another even though the multipliers had the same relative "pin-orientation". Furthermore, the removal of two photomultipliers had no effect on the signal of the remaining photomultiplier. The graph of the signal versus telescope orientation did not change with time, as this was checked several times over a period of a few days.

The method, therefore, of removing the effect of the magnetic field from the signals obtained from an astronomical object was to calibrate the photomultipliers for each particular telescope orientation. This was done after each night's observations, using the neon lamp as a light source.

Mu-metal cans have been ordered but in view of previous work the author believes that the photomultipliers will still need to be calibrated after each night's observations, especially if real changes in the signals of the order of a per cent are to be detected. The above method of calibration is shown to be perfectly satisfactory by the results obtained at the telescope, described in the next section.

SECTION IV

RESULTS AND DISCUSSION

The results obtained at the telescope with the three beam photoelectric photometer are divided into three sections: (i) eclipse measurements, (ii) non-eclipse measurements, and (iii) star measurements, and an attempt is made to explain any discrepancies. Useful observations on the Moon were carried out on four nights - June 24th, 25th, 30th and July 1st, 1964, one of these being the night of total eclipse, i.e. June 25th.

Lunar Eclipse Measurements

One of the most serious problems in the photometry of a lunar eclipse is that the measurements of the brightness of a particular area of the Moon's surface that is being followed through the Earth's shadow may be affected by light scattered from the uneclipsed lunar surface. In order to compute the effect of the scattered light on the eclipsed portion of the Moon it was intended to follow continuously several well separated points on the lunar surface.

Comparison with previous work on lunar eclipses (16, 17, 18, 19)

showed that the expected factoral decrease in the three signals - green ($\lambda 5450 \text{Å}$), red ($\lambda 6714 \text{Å}$) and infra-red ($\lambda 7889 \text{Å}$) would be approximately 10^5, 10^4, 10^3, respectively. Measurements taken on the night immediately preceding the night of the eclipse showed that there would be sufficient illumination during totality for the eclipse to be observed in three colours simultaneously, the expected signal in each case being well above the dark current level of the photomultiplier. Extinction measurements taken on the night of June 24th were used to extrapolate the eclipse measurements to zero air mass. In this way it was hoped to confirm the well-known reddening of the Moon during an eclipse and to see if this reddening could be attributed, in part at least, to a luminescence band similar to the one shown in Figure 1, as no previous eclipse measurements appear to have been made in the infra-red at $\lambda 7889 \text{Å}$.

The weather conditions on both June 24th and June 25th were similar. On the night of June 24th the level of the mist descended leaving a clear sky and extinction measurements were taken on Sinus Iridum (45° N, 28° W). As the Moon was low in the sky (Declination - South 22° 15') and as previous

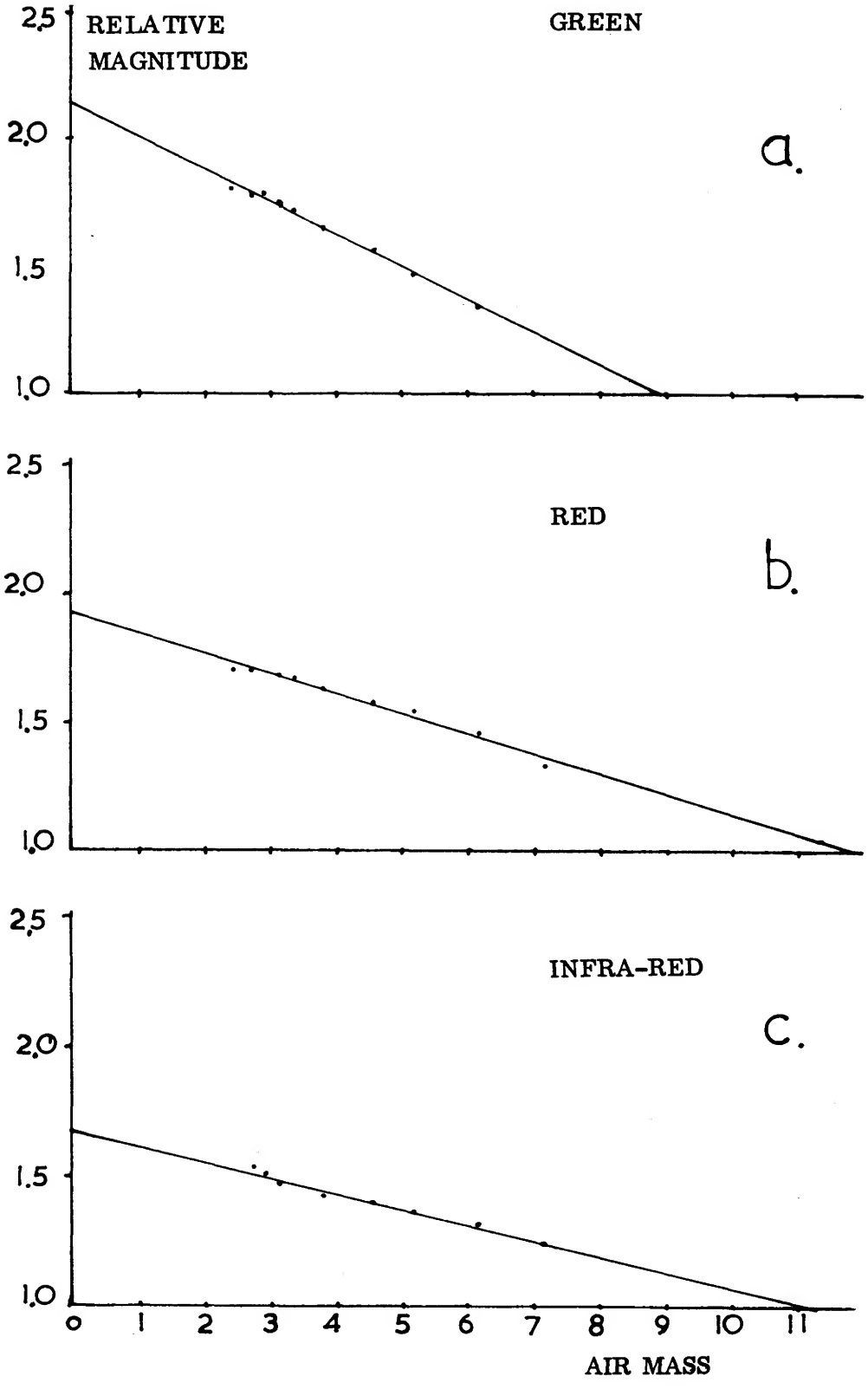

Figure 14

ATMOSPHERIC EXTINCTION CURVES, JUNE 24,1964.

bad weather had prevented extinction measurements on stars, it was decided that unless many values could be obtained with stars, then measurements taken on the Moon would be more accurate than extrapolating a few star measurements to large air mass values. It turned out that poor weather prevented further extinction measurements on stars and the extinction curves computed from Sinus Iridum readings were used to correct the eclipse measurements.

The extinction measurements, expressed in magnitudes, along with the air mass values calculated for the Pic-du-Midi, are combined to give the extinction curves shown in Figures 14a, b and c. The slope of the curve of magnitude against air mass, $\frac{\Delta m}{\Delta X}$, gives the extinction coefficient K, and the values of $K_G = 0.12$, $K_R = 0.08$ and $K_{IR} = 0.06$, for the extinction coefficients in the green, red and infra-red, respectively, compare favourably with the values obtained at other high altitude observatories [Mt. Wilson (Abbot) and McDonald (Hiltner) (20)].

On the night of the eclipse the Pic-du-Midi was covered with thick mist which unfortunately did not disperse until about one hour after the middle

of the eclipse (01.07 U.T.). Observations began at 02.07 U.T., although there was some thin mist about, but had to be abandoned at 03.00 U.T. due to banks of high cloud.

Because of the weather conditions, the intended programme could not be carried out, but three different regions were observed continuously as they moved from the umbra to the penumbra. The three regions were:-

Near Gassendi	35° W, 15° S;	02.07 to 02.19 U.T.
Near Ptolemaeus	10° W, 10° S;	02.21 to 02.35 U.T.
Mare Tranquilitatis	20° E, 10° N;	02.36 to 03.00 U.T

These regions are indicated on the photograph of the Moon in Figure 15. In each case, the maximum focal plane aperture was used, the diameter corresponding to 70 seconds of arc on the lunar surface. The limb of the Moon was already well illuminated by the time readings had begun on the region near Gassendi, so all the readings were affected to the same extent by scattered light.

The light curves are shown in Figures 16, 17 and 18. Each value has been corrected for extinction and for the range changes of the amplifier. The changing effect of the magnetic field on the photomultipliers was negligible

Figure 15

AREAS STUDIED DURING THE ECLIPSE

during the period of observation.

Though observing conditions were not ideal, the light curves show some interesting effects. Firstly, the light curves for the region near Gassendi show a much steeper rise with time than for the two other regions. This is probably due to scattered light affecting the latter two regions more than in the case of the Gassendi region. The readings for Mare Tranquilitatis were started when this region was well inside the umbra, thus, the curves show little change to start with, the slight change being due probably to an increase in the scattered light component. As the edge of the umbra passes through this region the illumination changes much more rapidly, giving rise to the steep slope of the light curves at 02.46 U.T.

Secondly, the light curves for the different colours cross each other at different times. In the case of the Gassendi region the infra-red curve crosses the red and green curves at 02.15 U.T. This effect is undoubtedly a cloud effect, for subsequent observations (following sections) showed that the infra-red signal was more affected by cloud than the red and green signals. This fits in with the behaviour shown in Figure 16 because the green and red curves show little change relative to each other whereas the infra-red curve

shows a definite decrease in the intensity of the infra-red light. The curves for the regions near Ptolemaeus and Mare Tranquilitatis confirm that this behaviour is a cloud effect and not a penumbral effect.

The crossing of the green and red light curves in Figures 17 and 18, when both regions were in the umbra, suggests that this is an effect peculiar to the umbra rather than a cloud effect. Furthermore, the red and infra-red curves show the same relative behaviour suggesting that only the green curve is affected. The phenomenon is probably caused by scattered light from the penumbra.

Further evidence for this suggestion comes from a paper by Reaves and Walker (18) on the photoelectric photometry of the lunar eclipse of September 26th, 1950. Observations made by them in the green (λ5350 Å) and in the blue (λ4230 Å) showed that the green and blue light curves crossed just inside the umbra and recrossed when further in the umbra; in a similar fashion to the red and green curves in Figures 17 and 18. Comparison with their measurements (9) for the July 26th, 1953 eclipse, when the trailing limb of the Moon was followed into the eclipse to minimise the effect of scattered light, suggests that the crossing of the light curves during the 1950

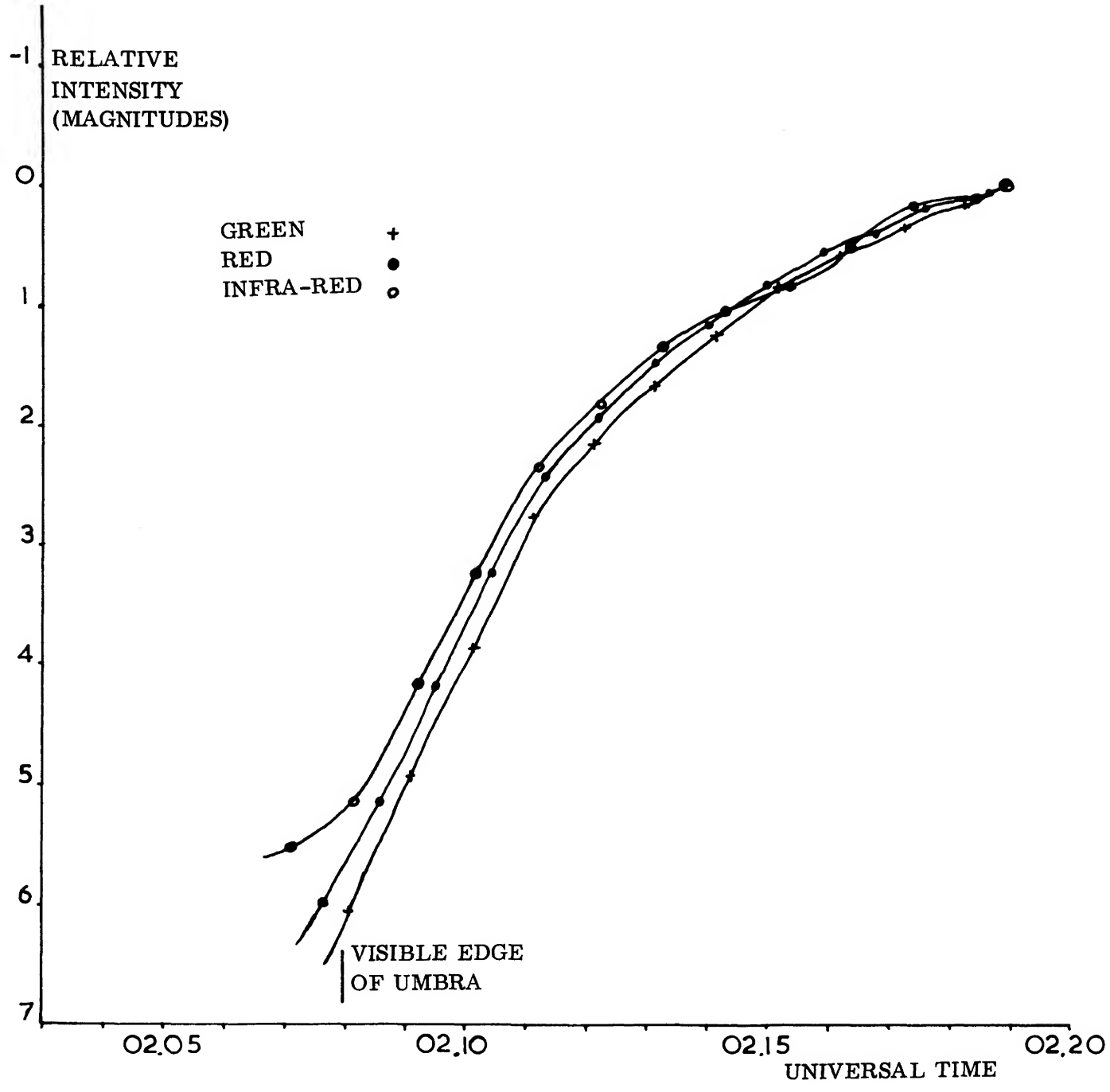

Figure 16

LIGHT CURVES FOR REGION NEAR

GASSENDI (35^{o}W 15^{o}S)

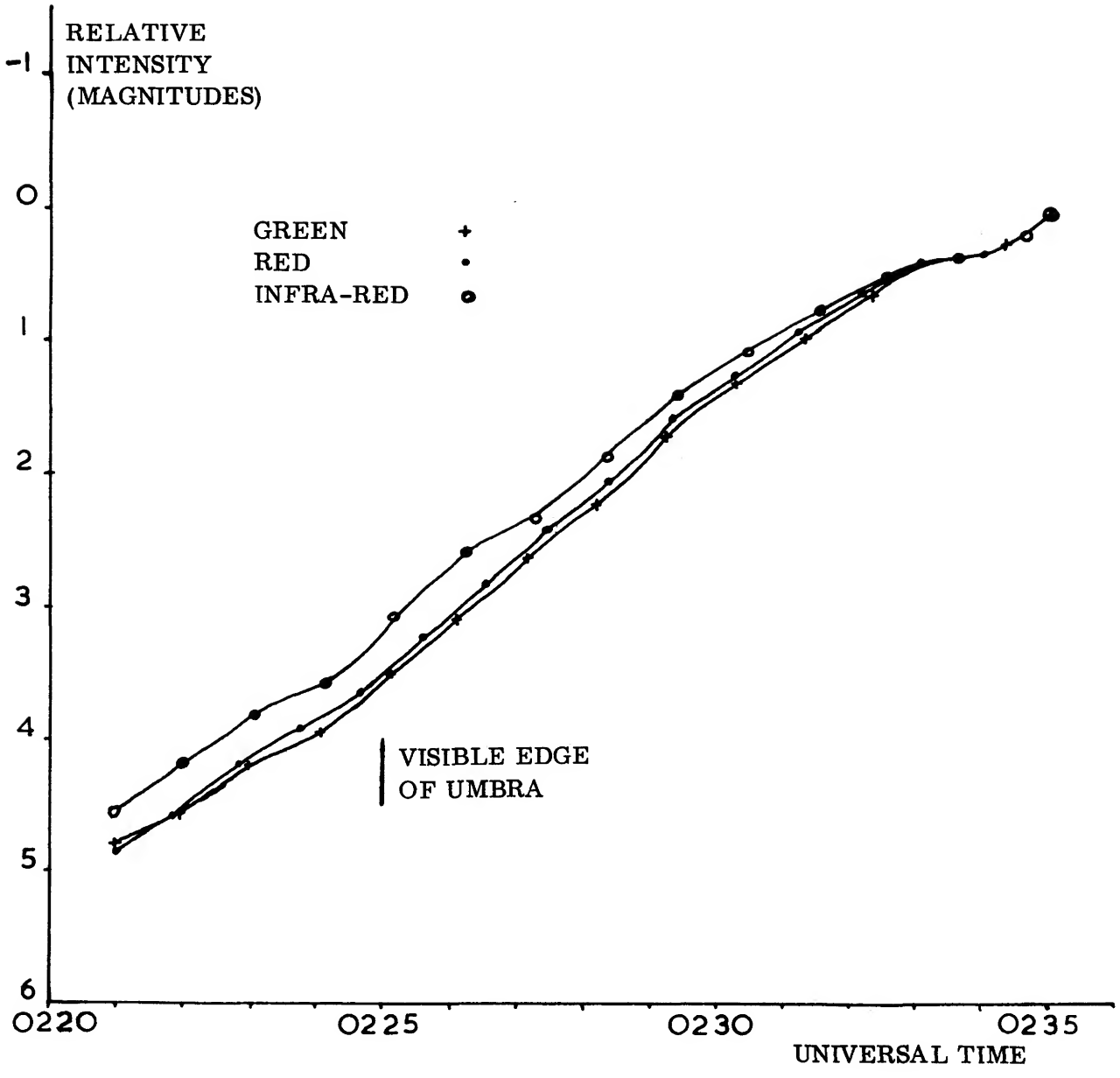

Figure 17

LIGHT CURVES FOR REGION NEAR

PTOLEMAEUS (10^{o}W 10^{o}S)

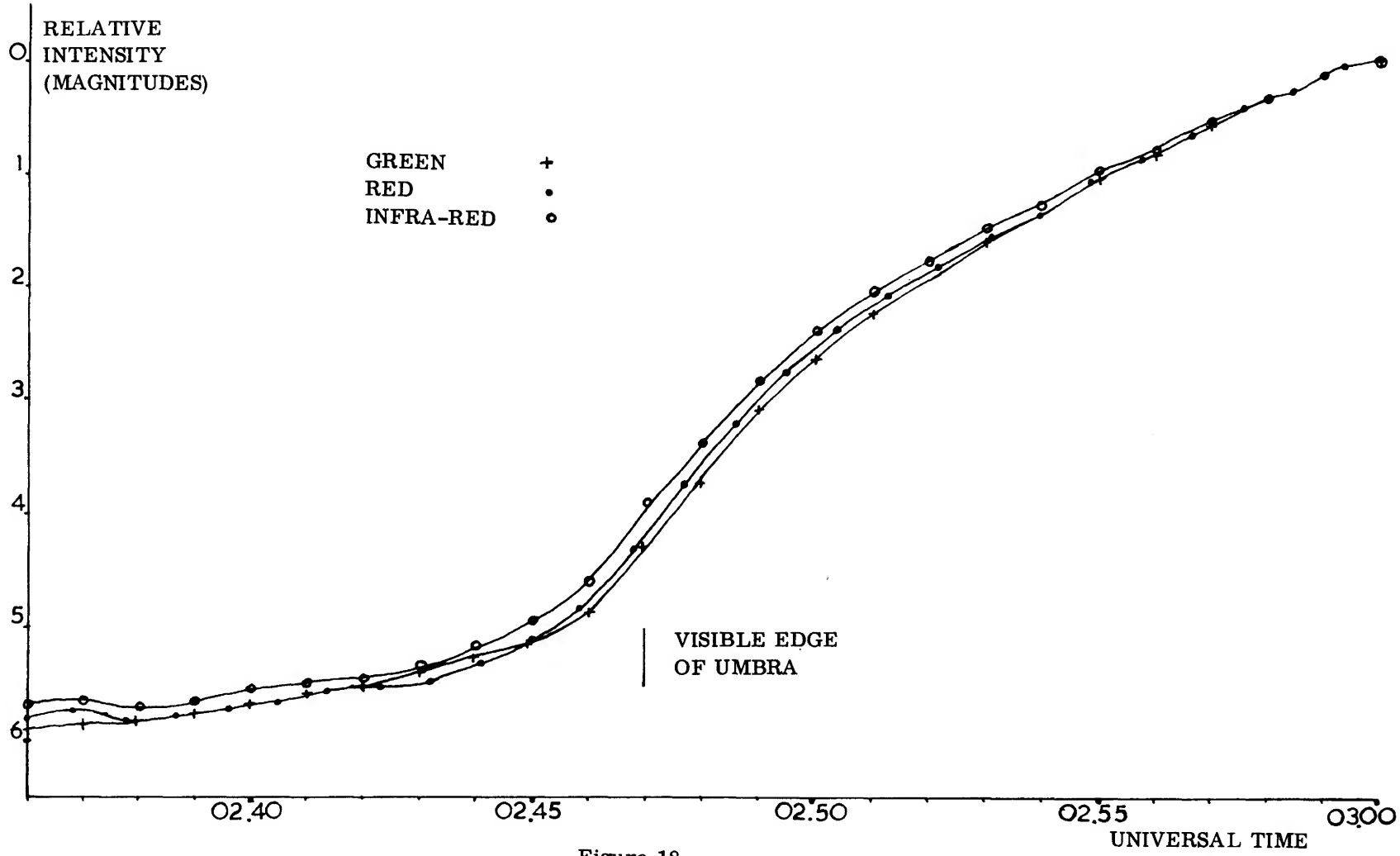

Figure 18

LIGHT CURVES OF REGION IN MARE TRANQUILLITATIS (20°E, 10°N)

eclipse was caused by scattered light. More observations, however, are needed before any definite conclusions about the crossing of the green and red light curves can be reached.

Thirdly, the green, red and infra-red light curves remain separated well into the penumbra, showing the well-known reddening of the Moon during an eclipse. In view of the observing conditions a detailed quantitative analysis of the results was not carried out, but a comparison of the light values in the umbra with those obtained the previous night shows that the red and infra-red signals both decreased by a factor approximately of 3×10^3 whereas the green signal decreased by a factor of approximately 2×10^4.

The red and infra-red signals were expected to decrease by different amounts and what was observed could have been either a lack of infra-red illumination caused by atmospheric absorption (cloud) or a red enhancement due to luminescence of the lunar surface. As it was not possible to follow the Moon during the complete period of the eclipse no definite conclusion can be reached, but in view of the observed effect of cloud on the infra-red signal it is more probable that the effect observed was atmospheric.

Non-eclipse Measurements

Measurements on the uneclipsed Moon were made on June 30th and July 1st, 1964, when the Moon was nineteen and twenty days old, respectively. The observing procedure was as follows.

A reading was taken in three colours simultaneously, say on Copernicus, the chart recorders were then stopped and the telescope guided into another region, say Kepler, and when in position the chart recorders were started simultaneously. This process was repeated for four regions - Kepler, Copernicus, Aristarchus and Sinus Iridum, the reading on each region taking about half an hour. The whole procedure was then repeated for the duration of the observing time.

Figure 19 shows the typical recordings obtained and Figure 20 shows the areas observed, with the diameter of the focal plane aperture corresponding to 50 seconds of arc on the lunar surface. The chart readings were corrected for the effect of the magnetic field on the photomultiplier, and the ratios of the red signal to the green and infra-red signals, respectively, were calculated. Tables 4.1 and 4.2 show the values of these ratios for the four regions observed during the two nights.

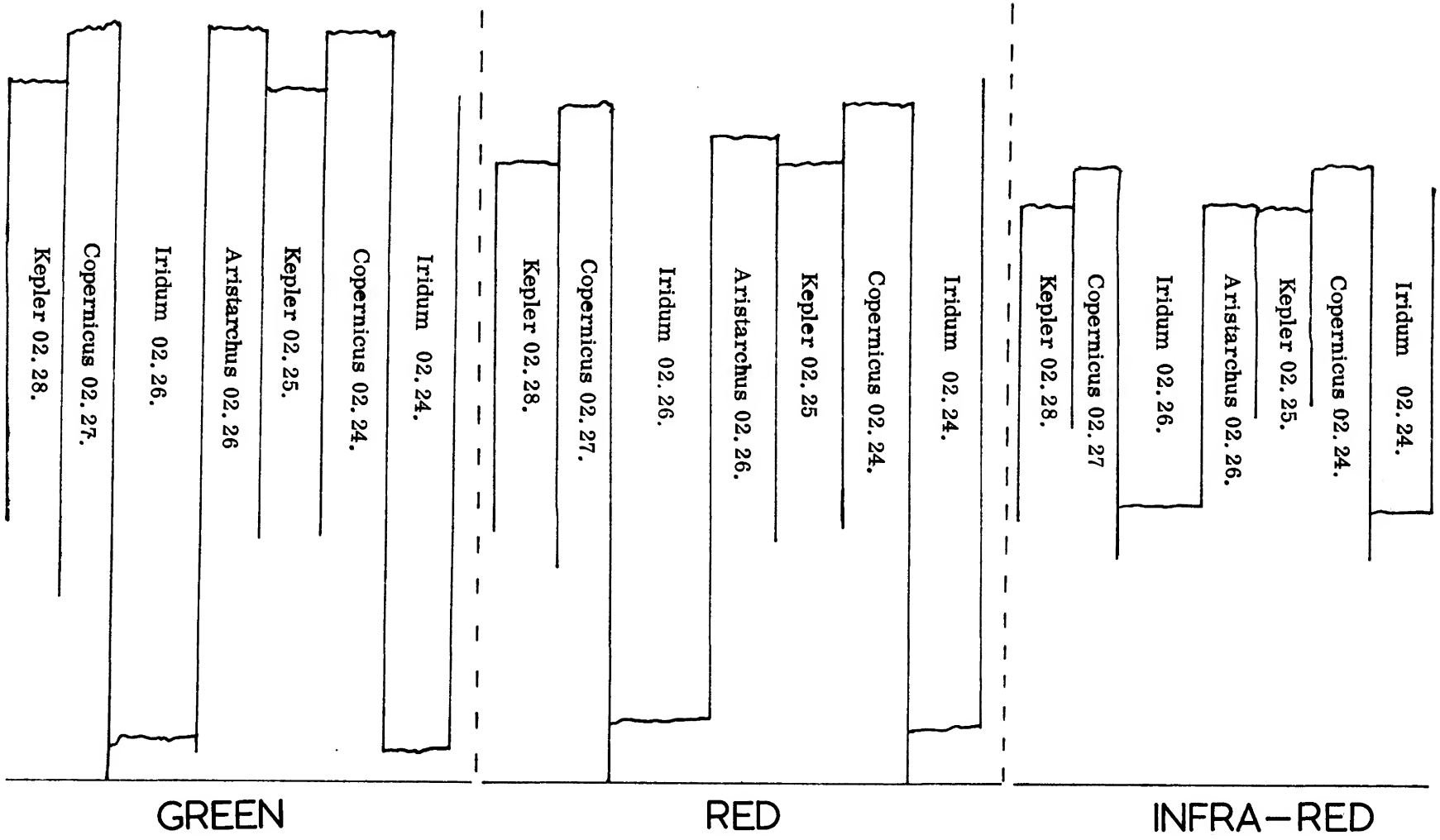

Figure 19

TYPICAL RECORDINGS.

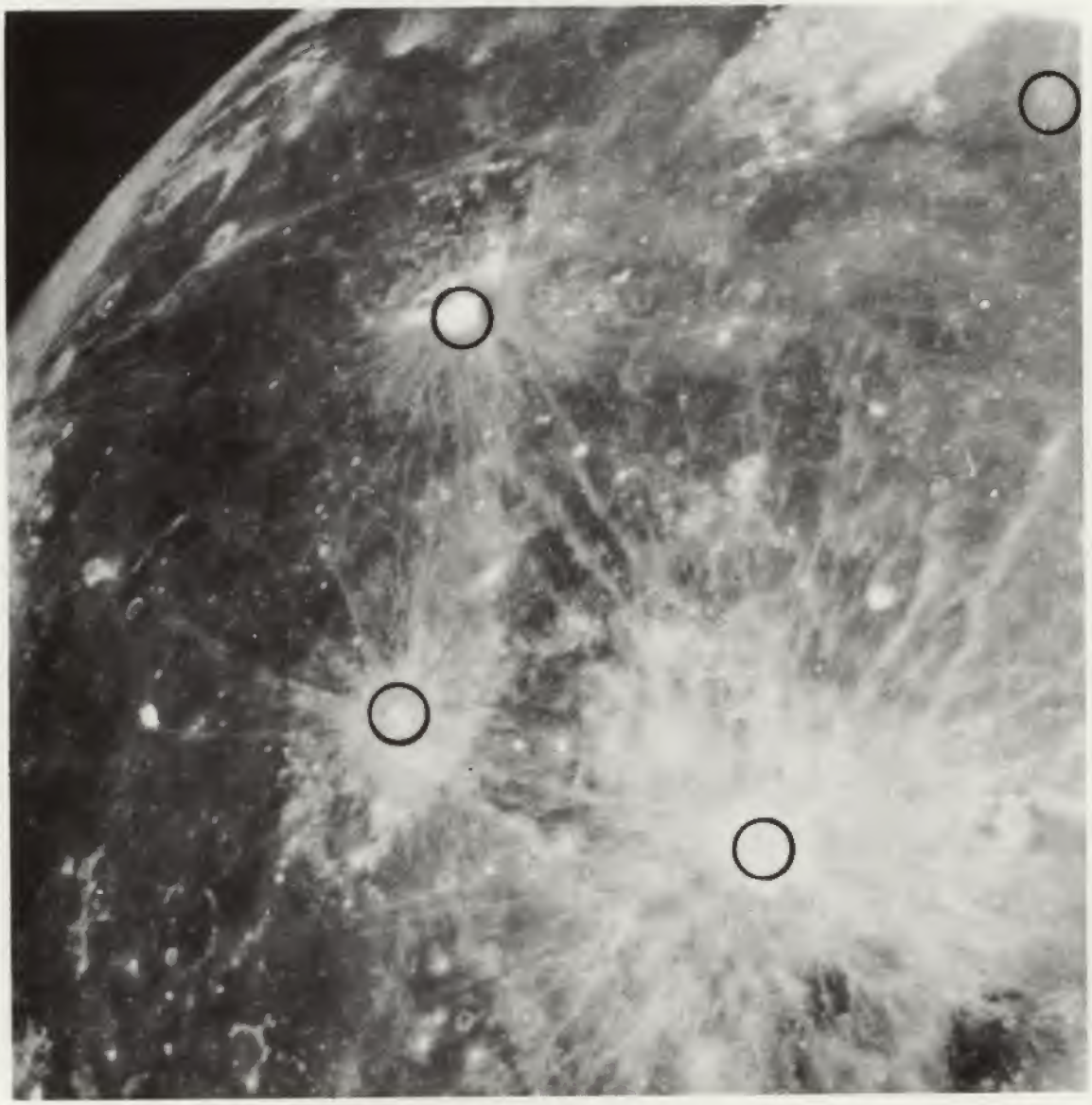

Figure 20

COPERNICUS, KEPLER, ARISTARCHUS AND SINUS IRIDUM

By the continuous observation of the four regions it was hoped to monitor any relative changes in the signals due to luminescence, Sinus Iridum being chosen as a reference area not likely to luminesce.

The results obtained on June 30th show that the $\frac{R}{G}$ $\left(\frac{\text{Red}}{\text{Green}}\right)$ values decrease steadily with time whereas the $\frac{R}{I.R.}$ $\left(\frac{\text{Red}}{\text{Infra-red}}\right)$ values increase steadily with time. Comparison with values obtained on July 1st shows that the $\frac{R}{G}$ values show a similar steady decrease with time, but no definite trend is shown for the $\frac{R}{I.R.}$ values. Table 4.4 summarises these changes and Table 4.3 summarises the different observing conditions for the two nights.

The differential change in the ratios with time is a manifestation of the different extinction coefficients for the three colours coupled with the change in air mass during the course of observations. This can be understood in the following way.

The intensity of the light emitted by an astronomical object is expressed ideally in terms of the intensity measured on the surface of the earth, as

TABLE 4.1

Moon Ratios

Copernicus			Kepler			Aristarchus			Sinus Iridum		
Time	$\frac{R}{G}$	$\frac{R}{I.R.}$	Time	$\frac{R}{G}$	$\frac{R}{I.R.}$	Time	$\frac{R}{G}$	$\frac{R}{I.R.}$	Time	$\frac{R}{G}$	$\frac{R}{I.R.}$
01.07	.94	1.14	01.07	.93	1.16	01.08	.91	1.18	01.09	.96	1.14
01.10	.94	1.15	01.11	.93	1.16	01.11	.91	1.18	01.12	.96	1.14
01.13	.93	1.15	01.14	.93	1.16	01.15	.91	1.18	01.16	.95	1.14
01.16	.93	1.15	01.17	.92	1.17	01.17	.90	1.19	01.18	.95	1.14
01.19	.93	1.15	01.20	.92	1.16	01.20	.90	1.18	01.21	.94	1.14
01.23	.92	1.15	01.24	.92	1.17	01.25	.90	1.19	01.25	-	-
01.26	.92	1.15	01.27	.91	1.17	01.28	.89	1.19	01.29	.94	1.15
01.29	.92	1.15	01.30	.91	1.17	01.31	.89	1.19	01.31	.94	1.15
01.32	.92	1.15	01.33	.91	1.17	01.33	.89	1.19	01.34	.94	1.15
01.35	.91	1.16	01.36	.91	1.17	01.36	.89	1.19	01.37	.93	1.14

TABLE 4.1 (Cont'd.)

Copernicus			Kepler			Aristarchus			Sinus Iridum		
Time	$\frac{R}{G}$	$\frac{R}{I.R.}$	Time	$\frac{R}{G}$	$\frac{R}{I.R.}$	Time	$\frac{R}{G}$	$\frac{R}{I.R.}$	Time	$\frac{R}{G}$	$\frac{R}{I.R.}$
01.38	.91	1.15	01.38	.90	1.17	01.39	.88	1.19	01.39	.93	1.15
01.40	.91	1.16	01.41	.90	1.17	01.42	.88	1.19	01.42	.93	1.15
01.43	.91	1.16	01.44	.90	1.17	01.44	.88	1.19	01.45	.93	1.15
01.57	.90	1.16	01.58	.89	1.18	01.59	.87	1.20	01.59	.92	1.15
02.00	.90	1.16	02.01	.89	1.18	02.01	.87	1.20	02.02	.92	1.15
02.03	.90	1.17	02.03	.89	1.18	02.04	.87	1.20	02.04	.91	1.15
02.05	.90	1.16	02.06	.89	1.18	02.06	.87	1.21	02.07	.92	1.16
02.08	.89	1.17	02.08	.89	1.19	02.09	.87	1.20	02.10	.91	1.16
02.11	.89	1.17	02.11	.89	1.19	02.12	.87	1.20	02.13	.91	1.16
02.14	.89	1.17	02.14	.88	1.19	02.15	.87	1.21	02.15	.91	1.17
02.16	.89	1.17	02.17	.89	1.19	02.17	.86	1.21	02.18	.91	1.17
02.19	.89	1.18	02.20	.89	1.19	02.20	.87	1.21	02.21	.91	1.17

TABLE 4.1 (Cont'd.)

Copernicus			Kepler			Aristarchus			Sinus Iridum		
Time	$\frac{R}{G}$	$\frac{R}{I.R.}$	Time	$\frac{R}{G}$	$\frac{R}{I.R.}$	Time	$\frac{R}{G}$	$\frac{R}{I.R.}$	Time	$\frac{R}{G}$	$\frac{R}{I.R.}$
02.21	.89	1.18	02.22	.89	1.20	02.23	.87	1.21	02.24	.91	1.17
02.24	.89	1.17	02.25	.88	1.19	02.26	.86	1.21	02.26	.90	1.17
02.29	.89	1.18	02.30	.88	1.19	02.30	.86	1.22	02.31	.91	1.18
02.32	.88	1.18	02.32	.88	1.20	02.32	.86	1.22	02.33	.90	1.17
02.34	.88	1.18	02.35	.88	1.20	02.35	.86	1.22	02.36	.90	1.17
02.37	.88	1.18	02.37	.88	1.20	02.38	.85	1.21	02.38	.90	1.17
02.39	.88	1.18	02.40	.87	1.20	02.41	.85	1.22	02.41	.90	1.18

TABLE 4.2

Moon Ratios

Copernicus			Kepler			Aristarchus			Sinus Iridum		
Time	$\frac{R}{G}$	$\frac{R}{I.R.}$	Time	$\frac{R}{G}$	$\frac{R}{I.R.}$	Time	$\frac{R}{G}$	$\frac{R}{I.R.}$	Time	$\frac{R}{G}$	$\frac{R}{I.R.}$
01.42	1.08	1.79	01.43	1.08	1.77	01.40	1.06	1.85	01.41	1.10	1.76
01.45	1.08	1.79	01.46	1.08	1.76	01.43	1.06	1.85	01.44	1.09	1.77
01.48	1.08	1.80	01.49	1.07	1.75	01.46	1.06	1.84	01.47	1.09	1.77
01.52	1.08	1.80	01.52	1.07	1.76	01.50	1.05	1.85	Recorder	fault	
02.01	1.06	1.81	01.01	1.05	1.77	01.52	1.05	1.85	01.53	1.07	1.76
02.05	1.06	1.81	02.06	1.05	1.76	02.03	1.04	1.85	02.00	1.07	1.77
02.10	1.06	1.80	02.10	1.04	1.74	02.06	1.03	1.86	02.04	1.06	1.76
02.12	1.05	1.80	02.13	1.04	1.76	02.11	1.03	1.85	02.08	1.06	1.77
02.15	1.05	1.80	02.16	1.04	1.76	02.13	1.02	1.86	02.11	1.05	1.76
02.20	1.04	1.80	02.21	1.04	1.76	02.16	1.02	1.85	02.14	1.06	1.77

TABLE 4.2 (Cont'd.)

Copernicus			Kepler			Aristarchus			Sinus Iridum		
Time	$\frac{R}{G}$	$\frac{R}{I.R.}$	Time	$\frac{R}{G}$	$\frac{R}{I.R.}$	Time	$\frac{R}{G}$	$\frac{R}{I.R.}$	Time	$\frac{R}{G}$	
02.23	1.04	1.81	02.24	1.03	1.76	02.21	1.02	1.86	02.17	1.06	1.78
02.26	1.04	1.79	02.27	1.03	1.79	02.24	1.02	1.86	02.22	1.05	1.78
02.28	1.04	1.81	02.29	1.03	1.78	02.27	1.02	1.86	01.25	1.05	1.76
02.31	1.03	1.81	02.31	1.03	1.75	02.29	1.02	1.86	02.28	1.05	1.78
02.33	1.03	1.80	02.33	1.02	1.75	02.32	1.01	1.85	02.30	1.04	1.77
02.35	1.03	1.80	02.36	1.02	1.76	02.34	1.01	1.85	02.32	1.04	1.78
02.38	1.03	1.79	02.39	1.03	1.76	02.36	1.01	1.85	02.34	1.04	1.77
02.41	1.03	1.79	02.42	1.02	1.78	02.39	1.01	1.84	02.37	1.04	1.77
						02.42	1.01	1.84	02.40	1.04	1.76
									02.42	1.03	1.76

TABLE 4.3

	Observing Period	Hour Angle	Declination	Air Mass
30th June 1964	01.07 U.T.	43.25°	S 14°	2.83
	02.41 U.T.	20.60°	S 14°	2.00
1st July 1964	01.40 U.T.	46.30°	S 10°	2.63
	02.42 U.T.	31.30°	S 10°	2.01

TABLE 4.4

Percentage Changes in the Ratios

Date	Copernicus		Kepler		Aristarchus		Iridum	
	$\frac{R}{G}$	$\frac{R}{I.R.}$	$\frac{R}{G}$	$\frac{R}{I.R.}$	$\frac{R}{G}$	$\frac{R}{I.R.}$	$\frac{R}{G}$	$\frac{R}{I.R.}$
30/6/64	-6.4	+3.5	-6.5	+3.5	-6.6	+3.4	-6.3	+3.5
1/7/64	-4.6	-	-4.8	-	-4.7	-	-4.6	-

TABLE 4.5

Comparison of Values Obtained for the Two Nights for the Same Air Mass on Each Night

	30/6/64				1/7/64			
	Cop.	Kep.	Aris.	Irid.	Cop.	Kep.	Aris.	Irid.
Red	107.0	101.0	103.9	52.8	58.4	62.0	64.9	29.8
Green	103.0	97.8	102.1	49.7	56.2	60.2	63.9	28.6
Infra-red	62.6	58.5	59.1	31.1	32.3	34.9	35.0	16.8
$\frac{R}{G}$	1.04	1.04	1.02	1.06	1.04	1.03	1.02	1.05
$\frac{R}{I.R.}$	1.71	1.73	1.75	1.70	1.81	1.78	1.86	1.78

$$I = I_o e^{-\tau x}$$

where I is the measured intensity, I_o is the intensity of the light before passing through the atmosphere and τ is the absorption coefficient per unit length of the atmosphere. τ is a function of the wavelength (20), hence the ratio of the two measured intensities at wavelengths λ_1 and λ_2 at time t_1 is

$$\frac{I_{\lambda_1}(t_1)}{I_{\lambda_2}(t_1)} = \frac{I_{o\lambda_1}(t_1)}{I_{o\lambda_2}(t_1)} e^{-(\tau_1 - \tau_2)x_1} \qquad \left[\tau_1 \equiv \tau(\lambda_1) \text{ etc.} \right]$$

where x_1 is the thickness of the atmosphere through which the object is studied. At time t_2 the thickness of the atmosphere presented to the object is x_2, hence

$$\frac{I_{\lambda_1}(t_2)}{I_{\lambda_2}(t_2)} = \frac{I_{o\lambda_1}(t_2)}{I_{o\lambda_2}(t_2)} e^{-(\tau_1 - \tau_2)x_2}$$

If we assume the intensity of the light emitted by the object is constant, then

the change in the ratio, caused by the atmosphere, expressed as a fraction of the ratio at t_1, is

$$\frac{e^{-x_2(\tau_1 - \tau_2)}}{e^{-x_1(\tau_1 - \tau_2)}} - 1$$

$$= e^{-(x_2 - x_1)(\tau_1 - \tau_2)} - 1$$

Making the reasonable assumption that $(x_2 - x_1)(\tau_1 - \tau_2)$ is small, and using the expansion $e^y \sim 1 + y$ for small y, then the fractional change in the ratio is given by

$$(x_1 - x_2)(\tau_1 - \tau_2)$$

Now the air mass, X, is a direct measure of the thickness of the atmosphere and the extinction coefficient, K, is a direct measure of τ. Thus, the fractional change in the ratio is directly proportional to the change in air mass times the difference in extinction coefficients for the two colours.

For a given decrease in air mass the ratio $\frac{R}{G}$ will decrease whereas the ratio $\frac{R}{I.R.}$ will increase, the fractional changes being proportional to

the respective differences in the extinction coefficients. For a given ratio, the fractional change in the ratio is proportional to the change in the air mass.

These predictions are borne out fairly well in Table 4.4. With extinction coefficients of $K_G = 0.12$, $K_R = 0.08$ and $K_{I.R.} = 0.06$ (computed earlier) and $K_R - K_G = -0.04$ and $K_R - K_{I.R.} = +0.02$ then the ratio of the fractional change in $\frac{R}{G}$ of -6.5% to that in $\frac{R}{I.R.}$ of $+3.5\%$ (Table 4.4) obtained on June 30th, fits in fairly well with the ratio

$$\frac{K_R - K_G}{K_R - K_{I.R.}} = \frac{-0.04}{+0.02}$$

The ratio of the fractional change in the $\frac{R}{G}$ values, from one night to the other, of $\frac{6.4}{4.7} = 1.36$ shows a good correlation to the ratio of the change in air mass for the two nights of $\frac{0.83}{0.62} = 1.34$.

The $\frac{R}{I.R.}$ values show no definite trend on July 1st, even though the air mass changed by 0.62 and the $\frac{R}{G}$ values decreased by approximately

4.7% during the course of observations. On July 1st observations were made through thin high cloud which worsened as the observations progressed. Previous observations have shown that cloud has more effect on the infra-red signal than on the green and red signals. Observations on a star (next section) show that the fluctuations in the infra-red signal are greater than those in either the red or green signals.

It would appear, therefore, that the trend in the $\frac{R}{I.R.}$ values, observed on June 30th (when the sky was clear to the eye) was masked on July 1st by thin cloud. Even so the fluctuations in the $\frac{R}{I.R.}$ values are only of the order of a per cent.

Table 4.5 compares the values of $\frac{R}{G}$ and $\frac{R}{I.R.}$ on June 30th and July 1st for the same air mass (2.10) on each night (02.21 U.T. on June 30th and 02.29 U.T. on July 1st). The values on June 30th are obtained from the values in Table 4.1 by multiplying $\frac{R}{G}$ by 1.17 and $\frac{R}{I.R.}$ by 1.45. This correction has to be applied because the potentiometer arrangements between the amplifiers and the recorders were adjusted on June 30th to

accommodate the signals on the recorder scales. Table 4.5 also shows the corrected signals taken from the chart paper and it is obvious that the signals on June 30th were much higher than on July 1st - hence the potentiometer adjustment. The values of the readings of the individual signals in Table 4.5 give an idea of the decrease in the intensity of the measured signal over the two nights caused by the change in phase angle, and the decrease in atmospheric transparency on July 1st.

The values of $\frac{R}{G}$ for the same air mass on June 30th and July 1st are consistent to within 1% for the four regions observed, but on July 1st the $\frac{R}{I.R.}$ value shows an increase of approximately 5% over that for June 30th. This increase is almost certainly due to the decrease in the infra-red signal on July 1st caused by high cloud.

From the above discussion it can be said that the trend in the $\frac{R}{G}$ values is predictable and small, so a change in the ratio of 1%, caused by luminescence, would easily be detectable. In the absence of cloud, the same can be said for the $\frac{R}{I.R.}$ values.

In conclusion, therefore, it can be said that the fluctuations in the Moon-light, caused by luminescence, were certainly less than 1% during the periods of observations on June 30th and July 1st. Furthermore, the change in the ratio of the red to the green signal was less than 1% over a period of twenty-four hours suggesting that the luminescent component of the lunar light did not change appreciably over this period of time.

Coherency Checks

Measurements on the Moon (e.g. Figure 19) showed that the fluctuations in the signals in different colours, caused by the atmosphere, were coherent with time, but in poor observing conditions the fluctuations in the infra-red signal were higher than those in the red and green signals. Measurements made on a star (for which the scintillation is much greater than for the Moon) confirmed this. In the case of a star, the photometer was converted to measure the two wavelength regions simultaneously and Figure 21 shows the recordings made on the star Altair. The weather during the observations was windy and towards the end of the observations cloud interrupted readings.

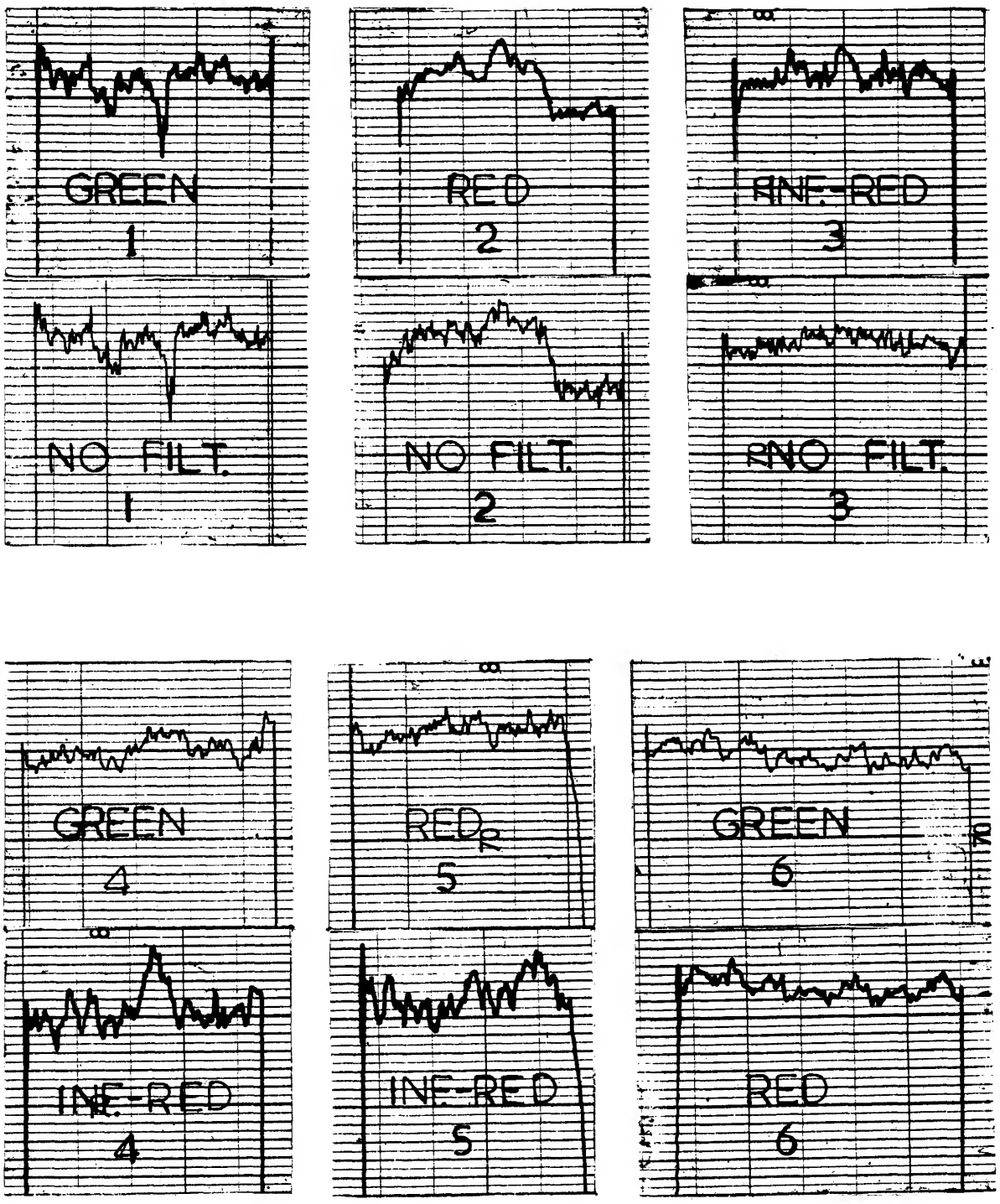

Figure 21

COHERENCY TESTS

Figure 21a shows that two signals when no filters were used and though the chart papers are moving at slightly different speeds, these show that the scintillation is coherent in the two beams (as expected) and is of the order of 7% of the signal.

Comparison with the other signals measured simultaneously shows that the scintillation in the green and red is coherent but the fluctuations in the infra-red signals are higher, especially when observed through cloud.

The fluctuations in the infra-red signal when cloud is present suggest that this signal is affected by the water vapour content of the atmosphere. A study of the Utrecht Atlas of the Solar Spectrum (21), however, shows only slight atmospheric absorption around λ 7810 Å, which is just within the transmission curve of the filter (Figure 2b).

Recent Improvements and Future Plans

Two chart recorders, capable of displaying the ratio of the red to green and red to infra-red signals, respectively, were shipped to France in December 1964 in preparation for the total eclipse of December 19th.

Cloud prevented observations during the eclipse and also prevented

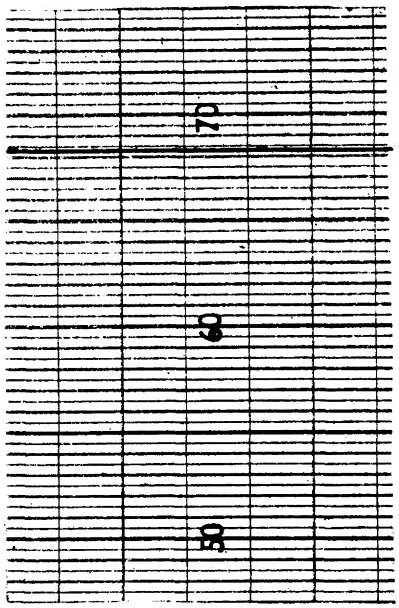

Ratio of Red to Green Signals

Ratio of Red to Infra-Red Signals

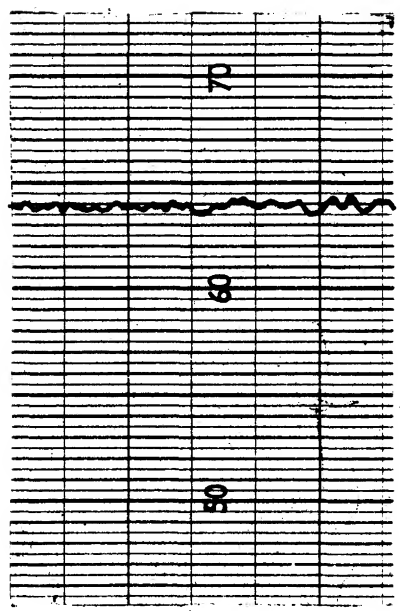

Figure 22

TYPICAL RATIO RECORDINGS FOR COPERNICUS

extensive observations during the following weeks. Observations, however, were carried out on December 20th, 1964 and Figure 22 shows typical recordings for the ratio of red to green and red to infra-red signals, respectively, for Copernicus. The red to infra-red shows the suspected effect of atmospheric water vapour on the infra-red signal. It is hoped that a new filter at $\lambda 7732 \text{Å}$ with a band width of 38Å, now available will eliminate this effect.

The results obtained so far have shown the capability of the three beam photoelectric photometer. In poor observing conditions the results show a consistency better than 1%. During the period of observations the fluctuation of the luminescent component of the lunar light was certainly less than 1% of the total light. This is not surprising in view of the fact that during the observing period telegrams were arriving at the Pic-du-Midi Observatory reporting periods of solar calm. However, the lunar measurements that have been obtained during this, the period of the "Quiet Sun" will serve as a useful reference during the coming years of increasing solar activity.

The immediate plan for future observations, therefore, is the

continued systematic measurement of the light from selected regions of the Moon, in three colours simultaneously. In this way it is hoped to correlate specific lunar events to specific solar events. It is hoped to carry out this programme from both the Pic-du-Midi and Helwan Observatories in France and Egypt, respectively. An immediate indication of the solar activity will be given in telegrams which will be sent from solar observing stations to both the Pic-du-Midi and Helwan Observatories.

REFERENCES

1. Link, F., Comptes Rendus, 223, 976, 1946
2. Kozyrev, N. A., Izv. Crim. Astr. Obs., 16, 148, 1956
3. Dubois, J., Journ. de Physique XVIII, 135, 1957
4. Grainger, J. F., Ph.D. Thesis, Manchester 1962
5. Derham, C. J. and Geake, J. E., Nature, 202, 62, 1964
6. Kopal, Z. and Rackham, T. W., Nature, 202, 171, 1964
7. Roberts, G. L., M.Sc. Thesis, Manchester 1964
8. Hiltner, W. A., The Observatory, 71, 234, 1951
9. Gehrels, T. and Teska, T. M., P.A.S.P., 72, 115, 1960
10. Derham, C. J., Geake, J. E. and Walker, G., Nature, 203, 134, 1964
11. Teifel, V. G., Soviet Astronomy, 3, 955, 1959 Original 36
12. Clarke, D., Ph.D. Thesis, Manchester 1963
13. Sharpe, J., Electronic Technology, June - July 1961 (E.M.I. Electronics Ltd.)
14. Lallemand, A., Astronomical Techniques, ed. Hiltner, W. A., p 154 (University of Chicago Press)
15. Eggen, D. J., "Photoelectric Studies VII" Ap.J., 114, 141, 1951
16. Link, F., "Physics and Astronomy of the Moon", Kopal, Z., pp 161 - 239 (Academic Press Inc. 1962)

17. Cuffey, J., Ap.J., 115, 17, 1952

18. Reaves, G. and Walker, M. F., P.A.S.P., 64, 15, 1952

19. Reaves, G. and Walker, M. F., P.A.S.P., 69, 153, 1957

20. Hardie, R. H., Astronomical Techniques, ed. Hiltner, W. A., p 185 (University of Chicago Press)

21. Delbouille, L., Roland, G., Photometric Atlas of the Solar Spectrum from λ7498Å to λ12,016Å (Inst. D'Astro. Univ. Liege)